

FIG. 1

U.S. DEPARTMENT OF THE INTERIOR

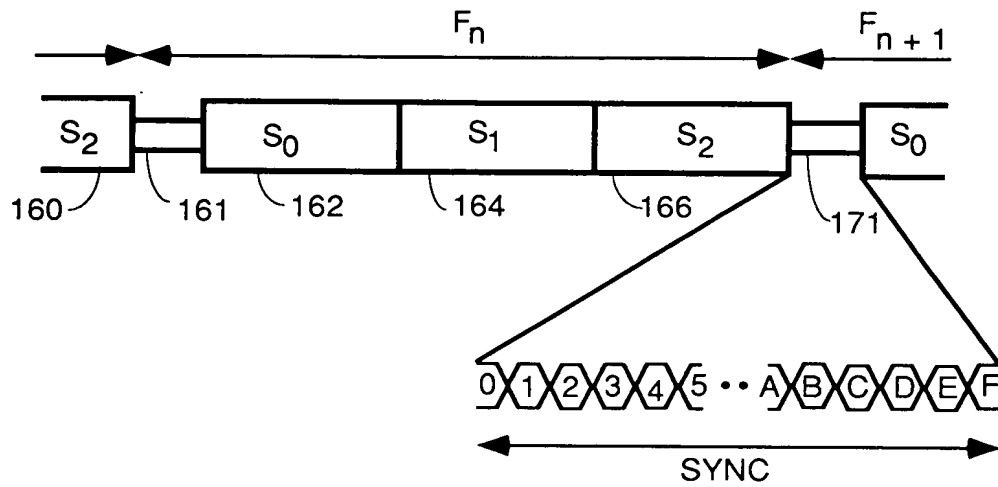


FIG. 2A

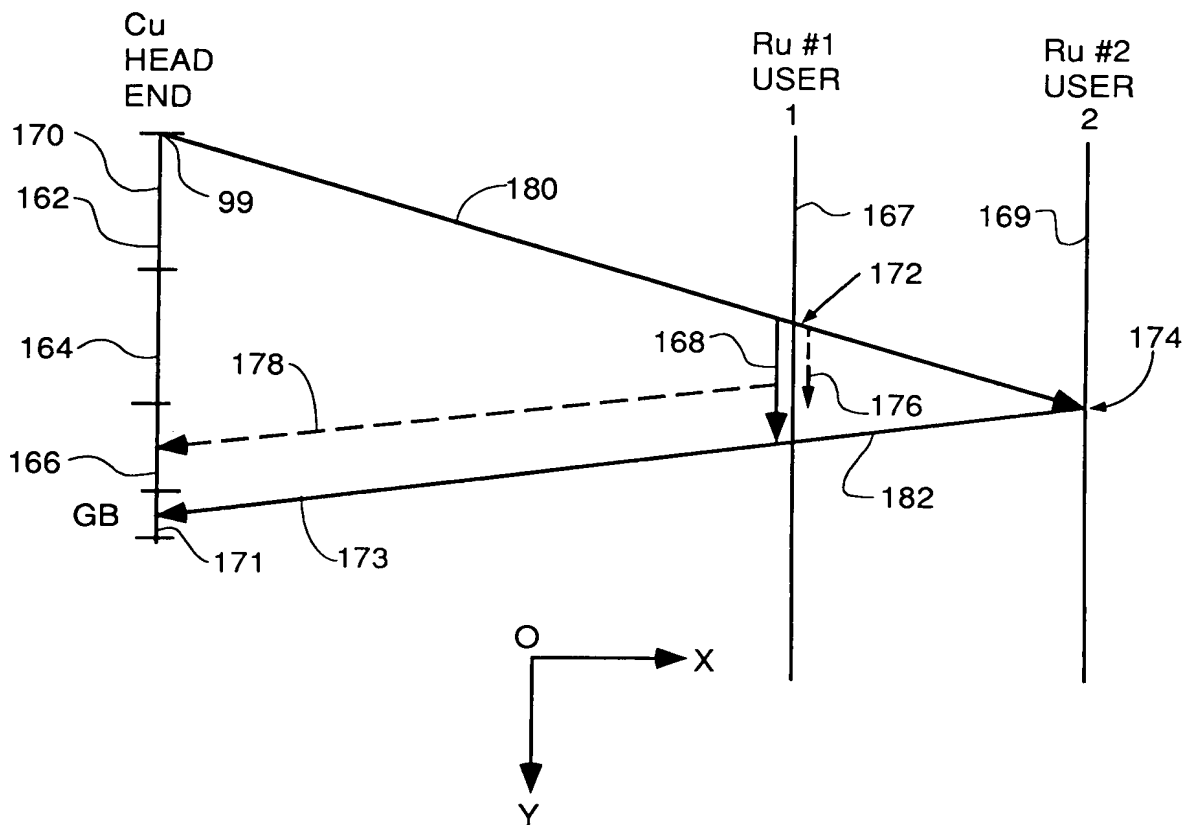


FIG. 2B

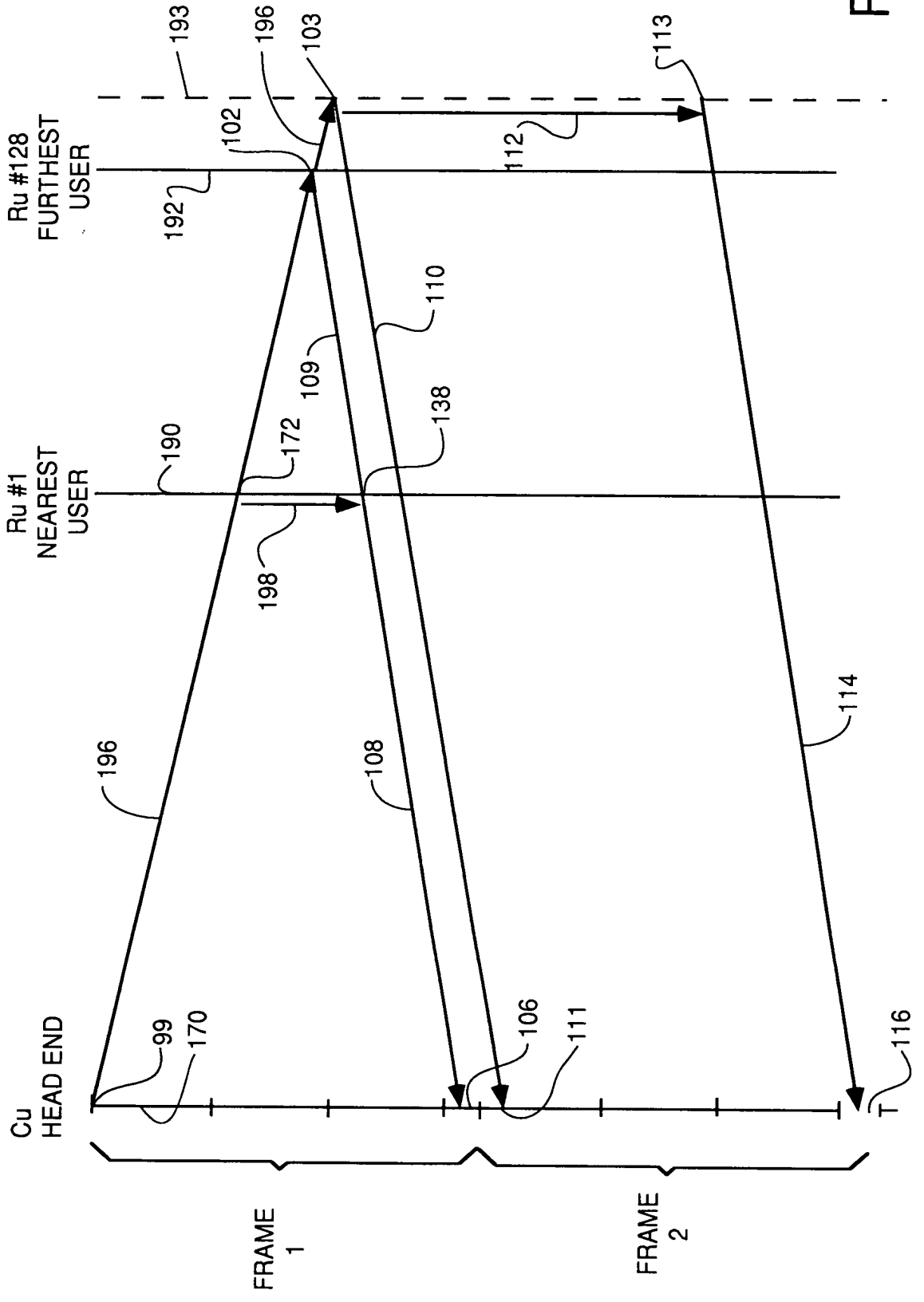
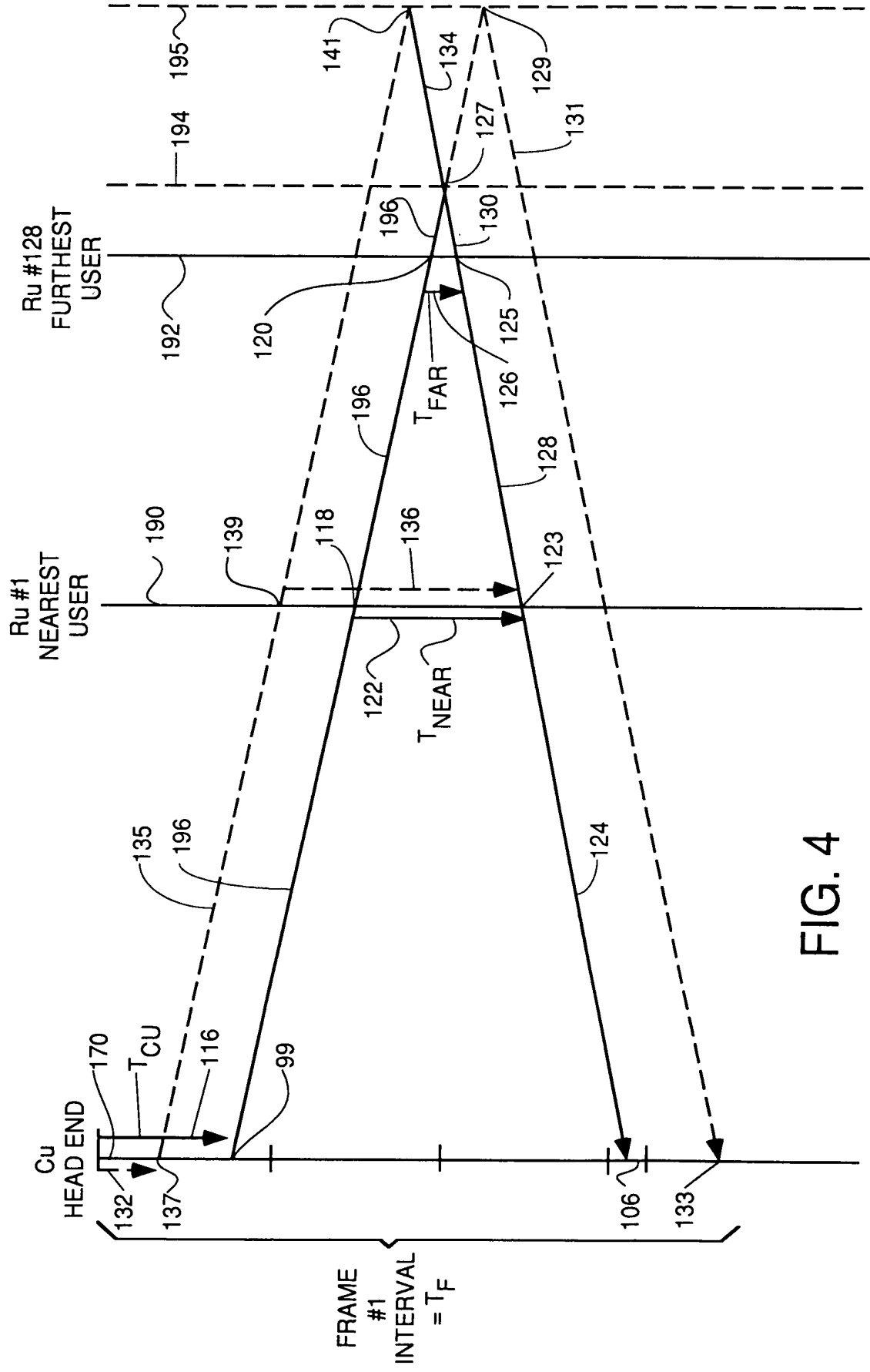
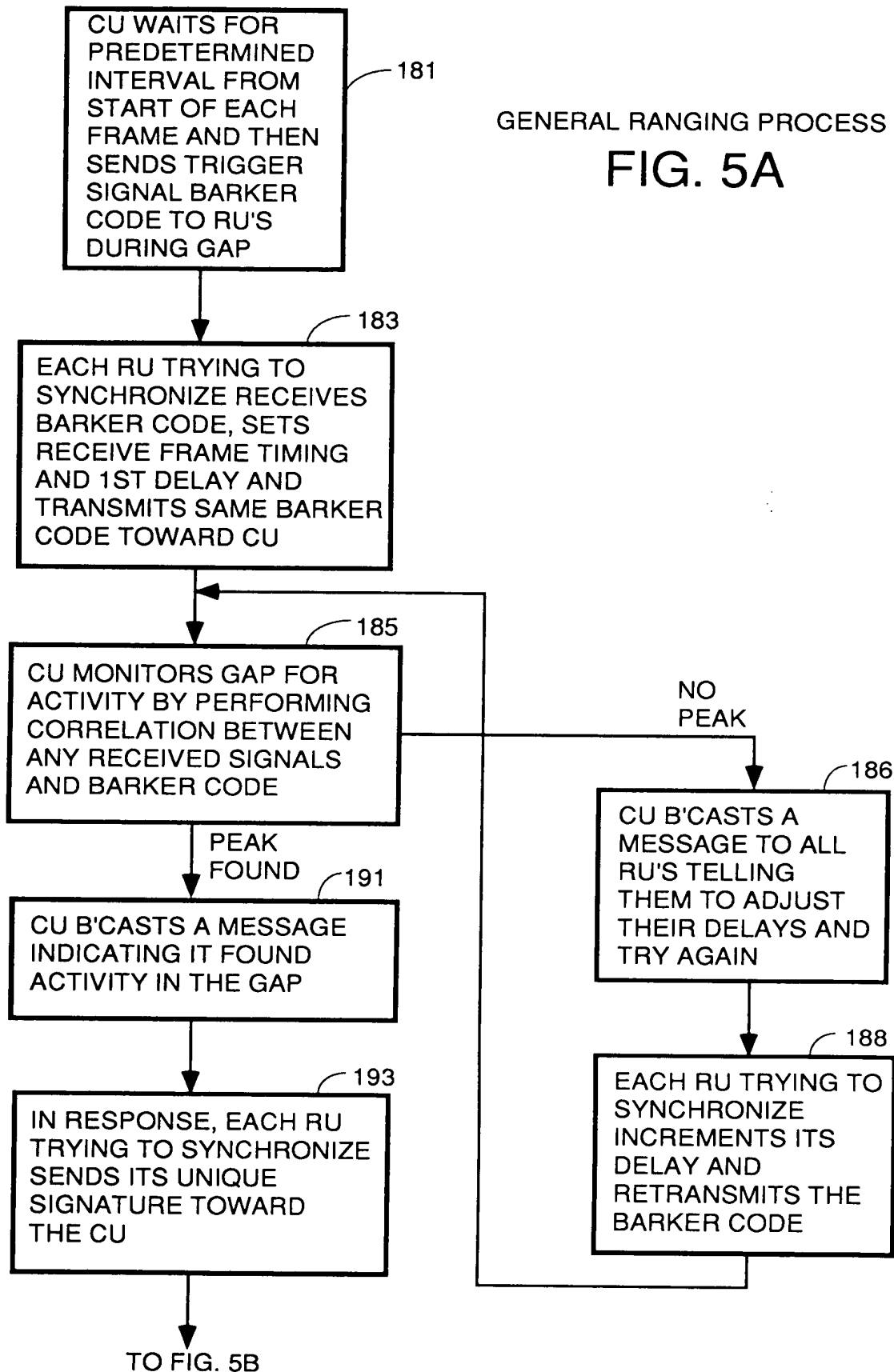


FIG. 3



GENERAL RANGING PROCESS

FIG. 5A



09759774-04301

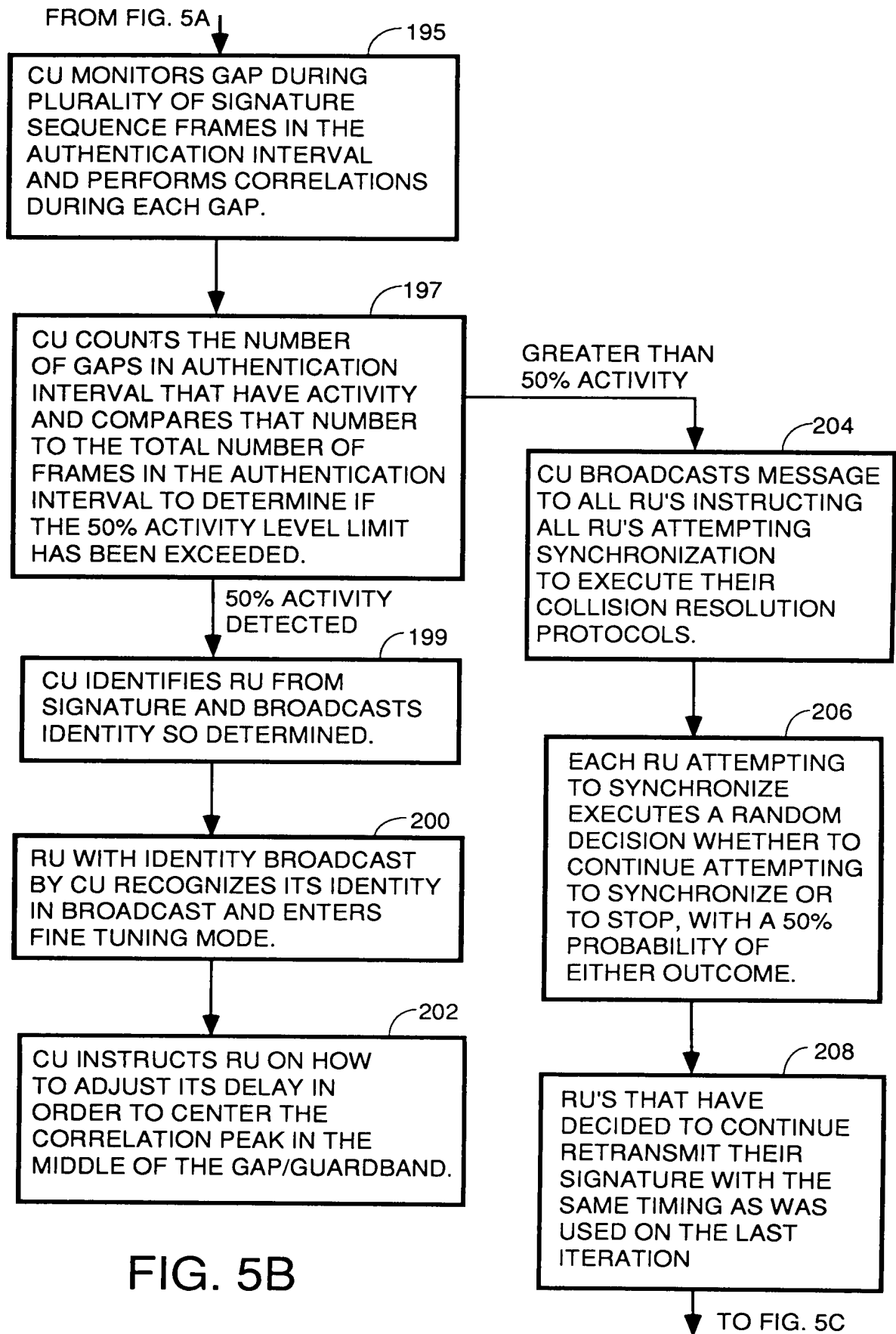


FIG. 5B

095974 04.10.01

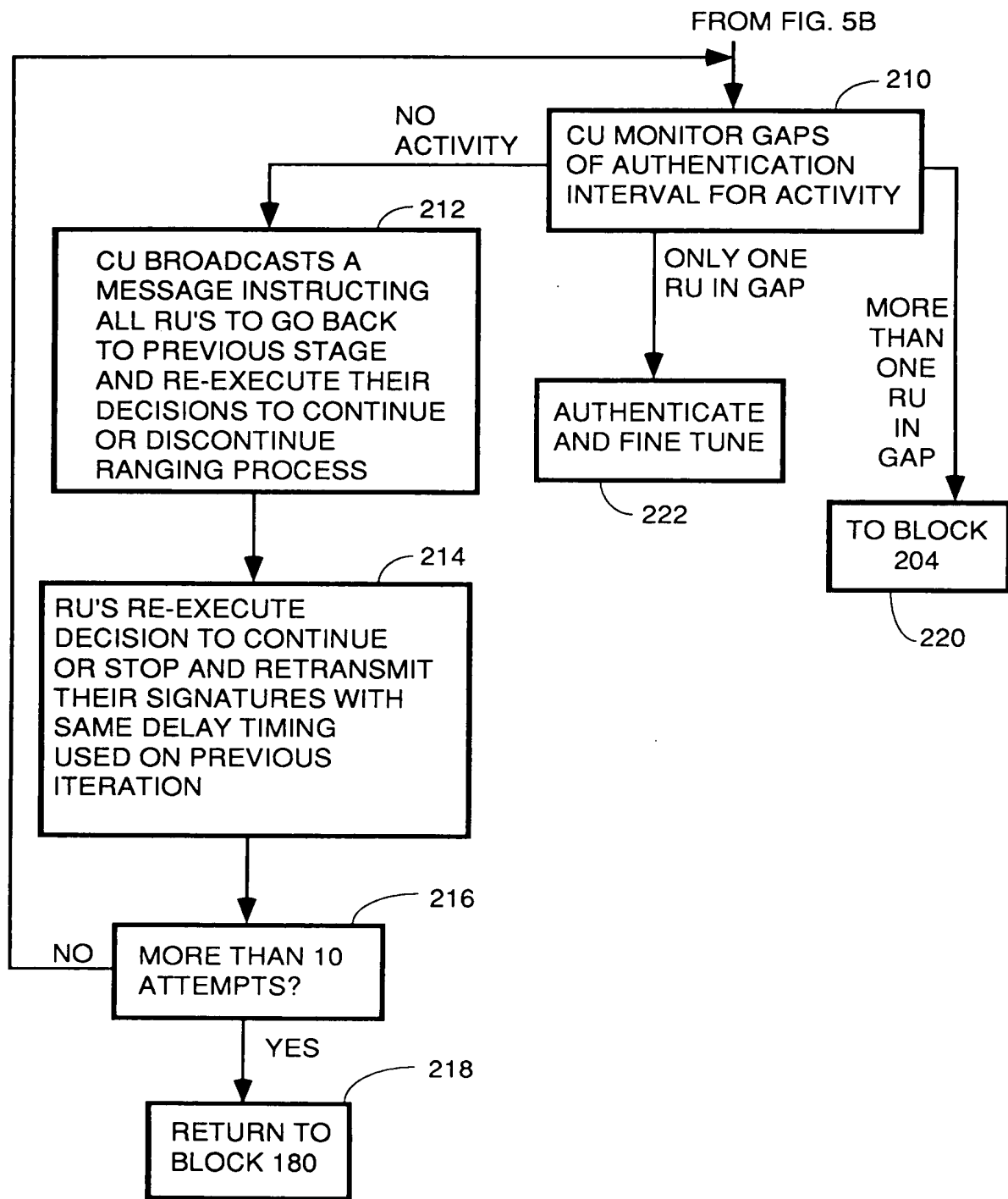


FIG. 5C

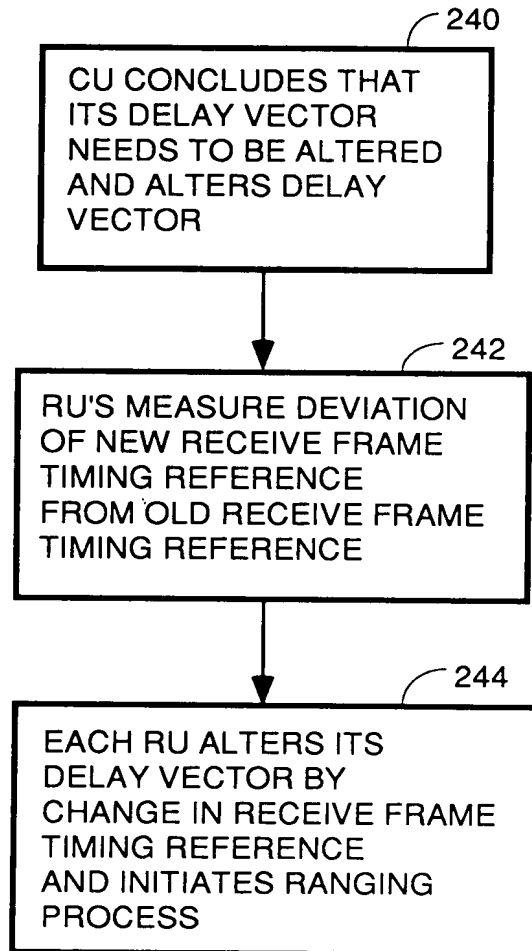


FIG. 6
DEAD RECKONING RE-SYNC

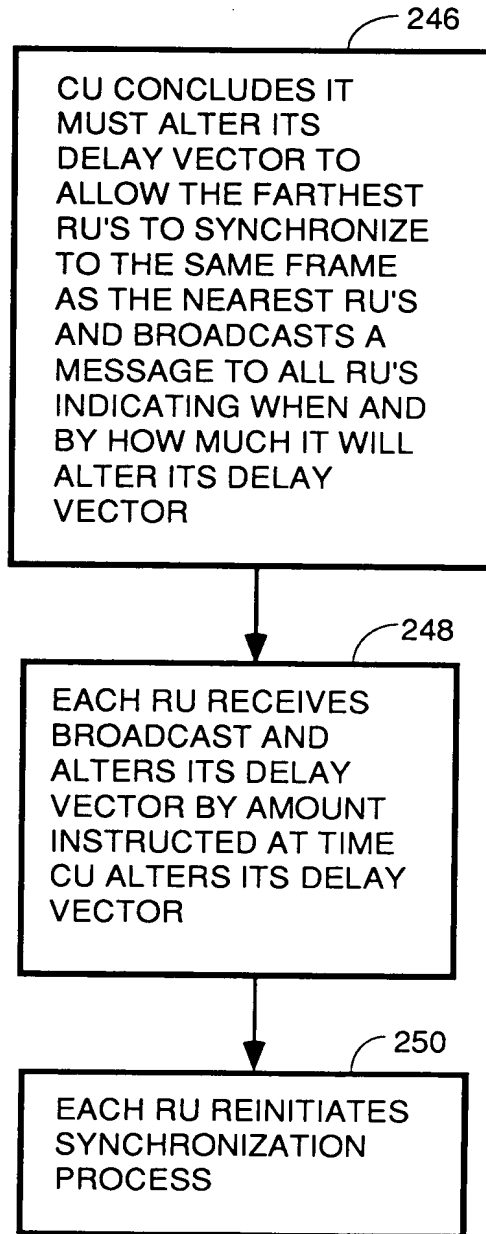
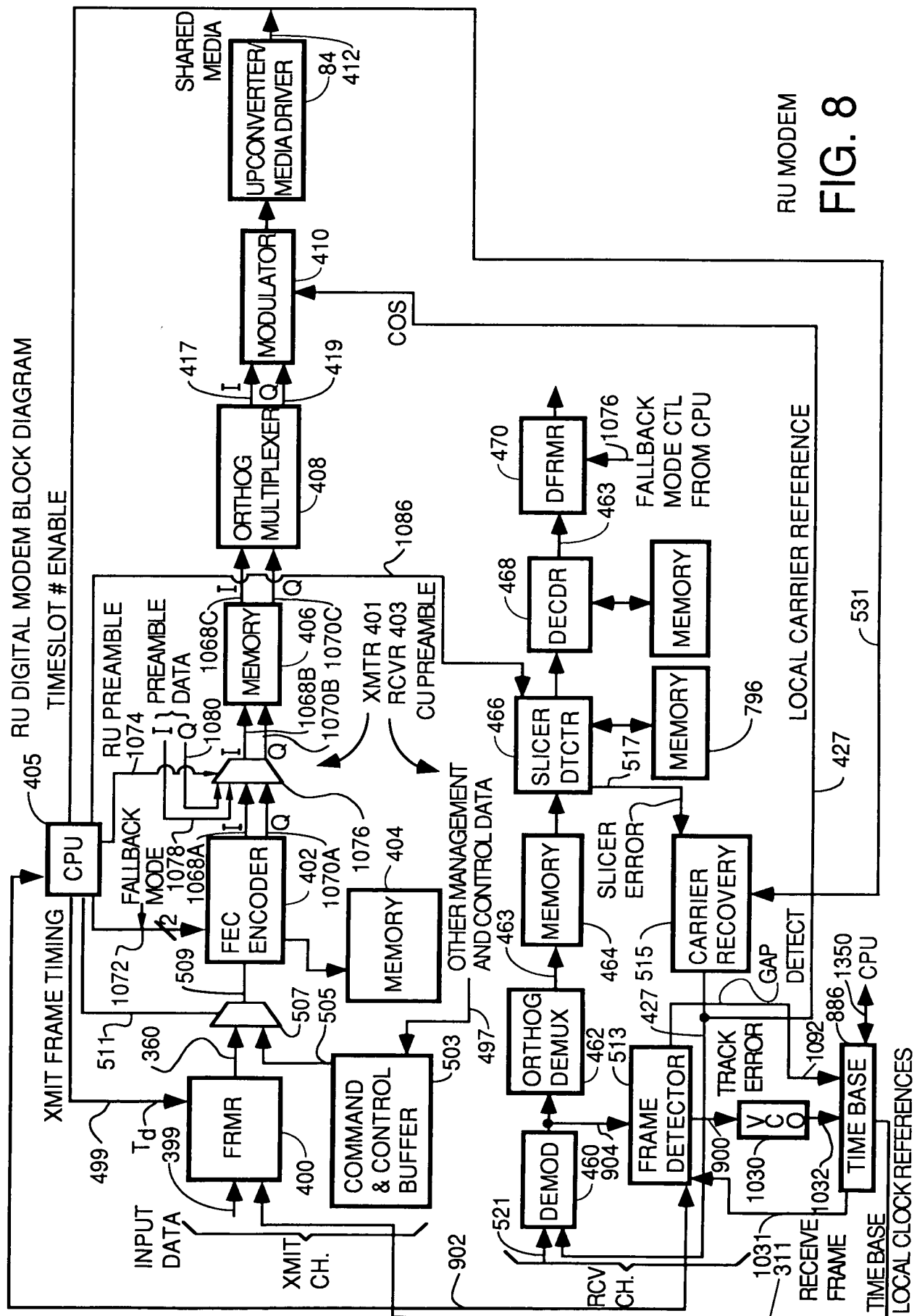


FIG. 7
PRECURSOR EMBODIMENT



RU MODEM
FIG. 8

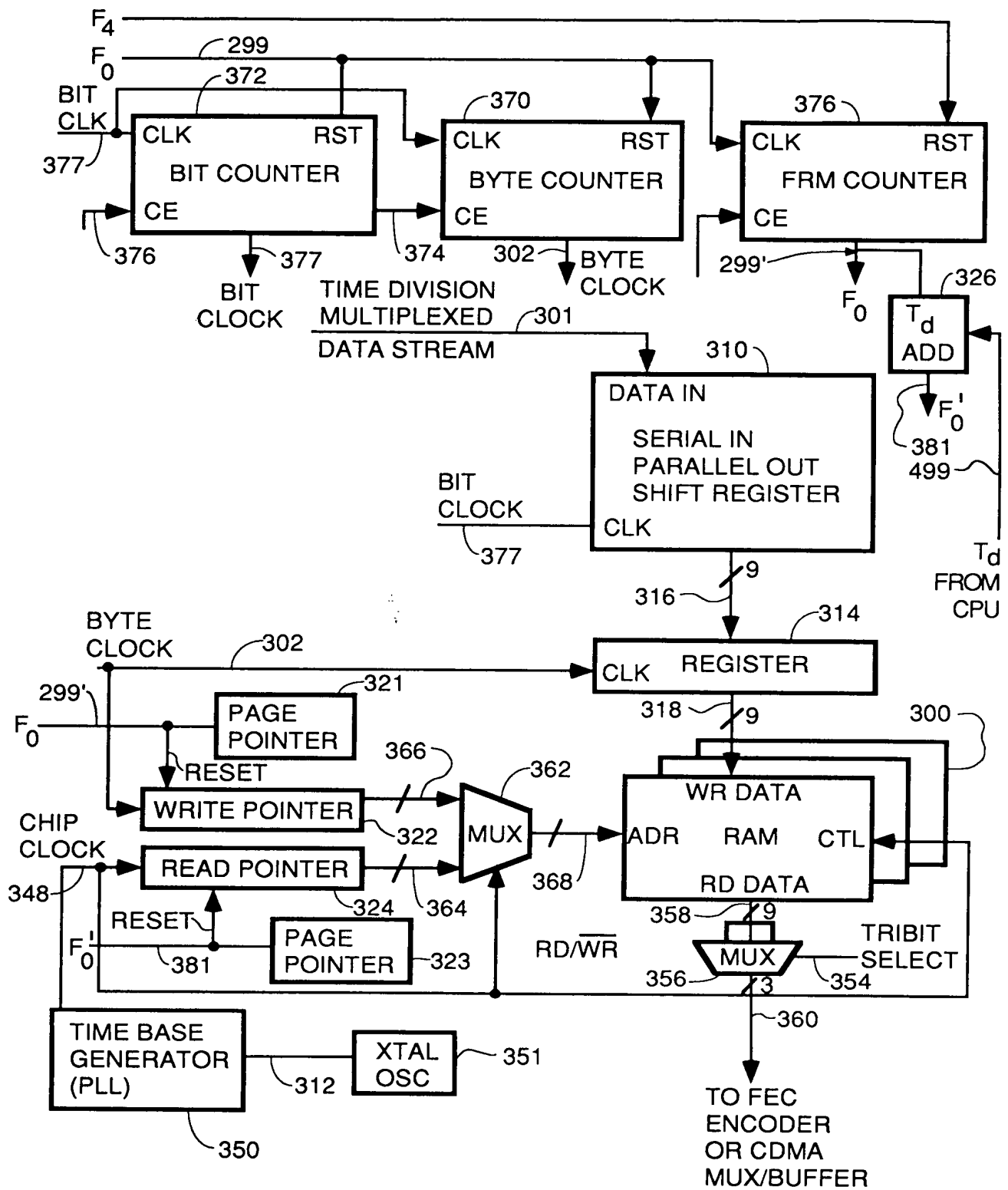


FIG. 9

0975974-04291

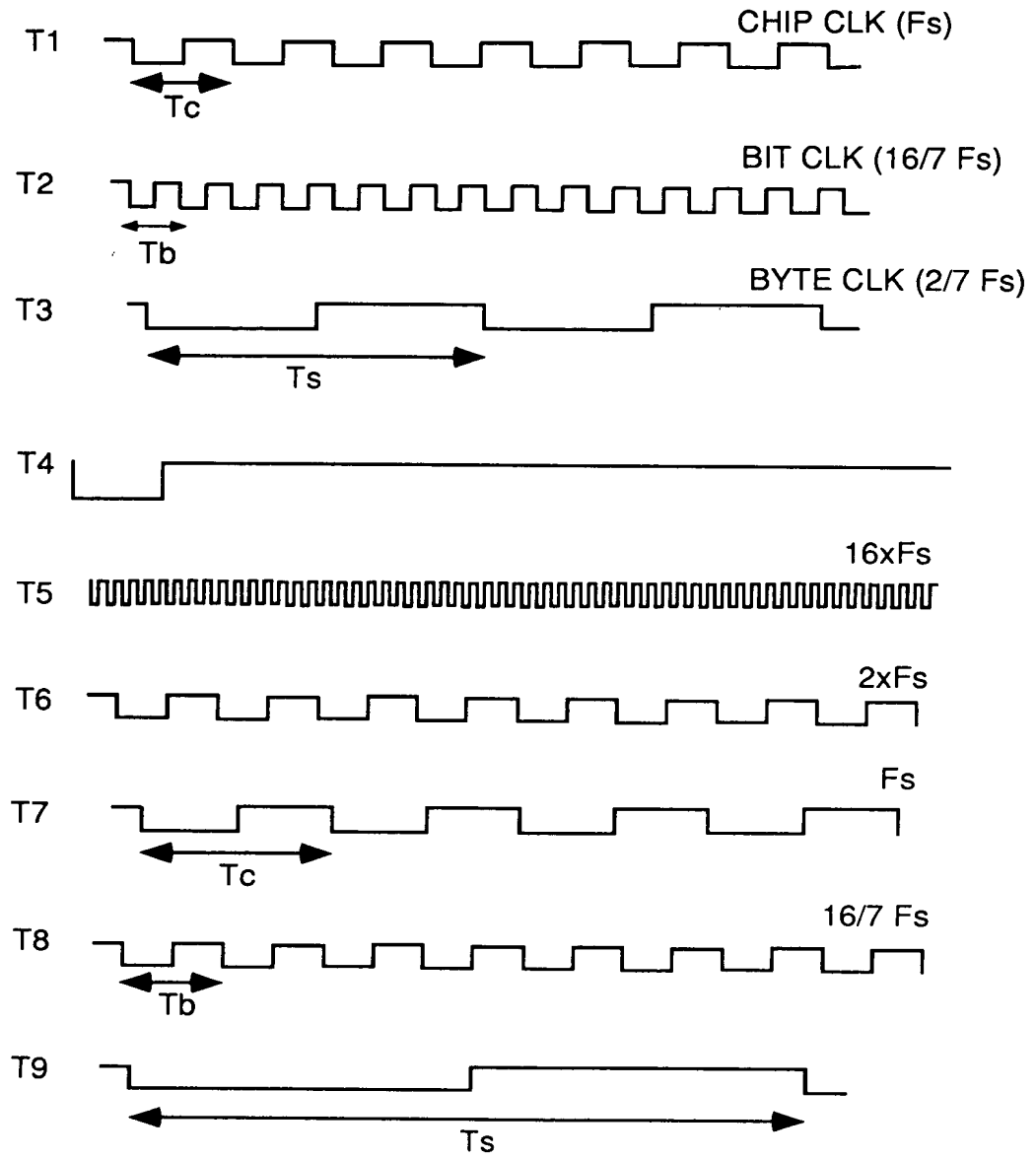


FIG. 10

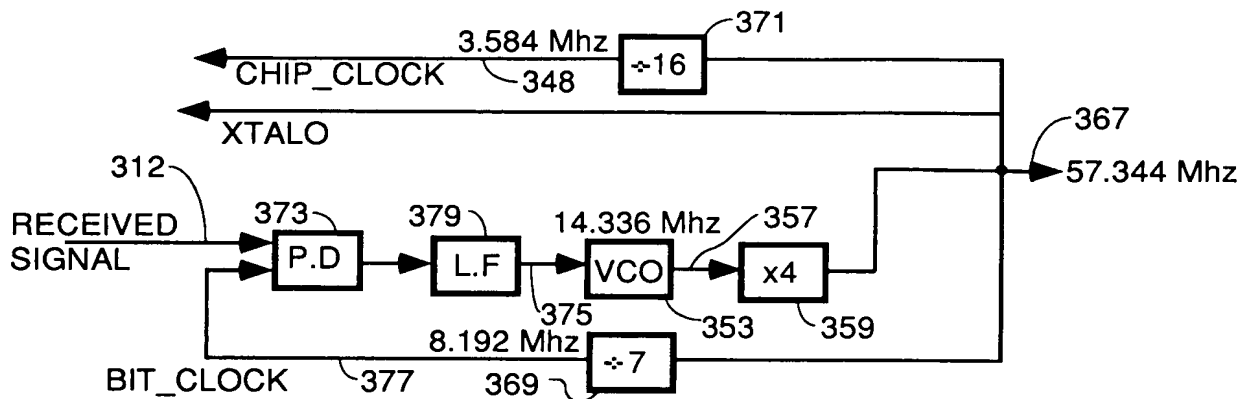


FIG. 11

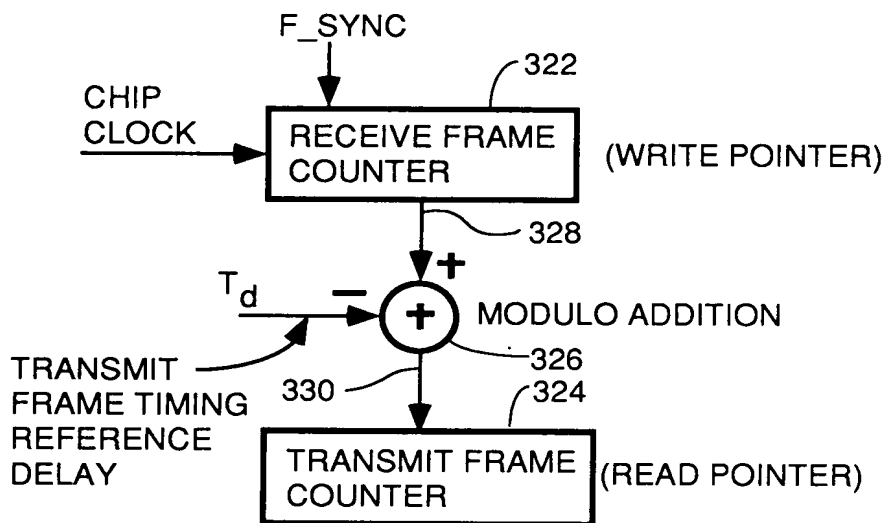


FIG. 12

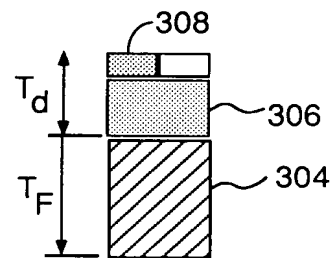


FIG. 13

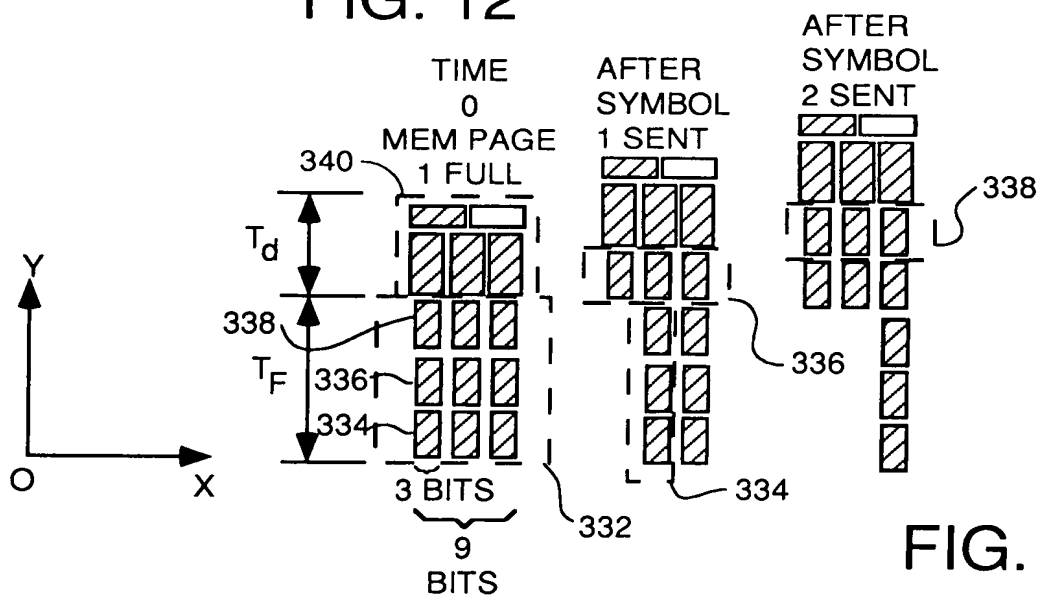


FIG. 14

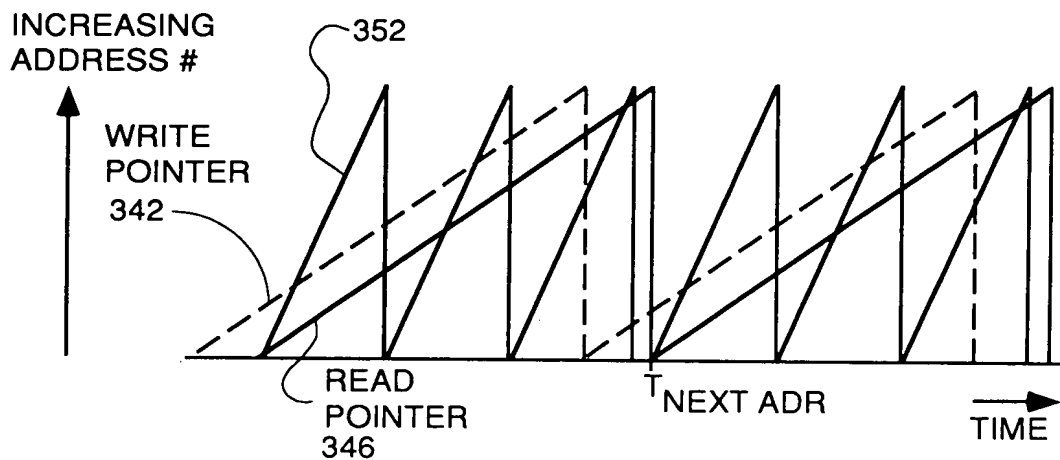


FIG. 15

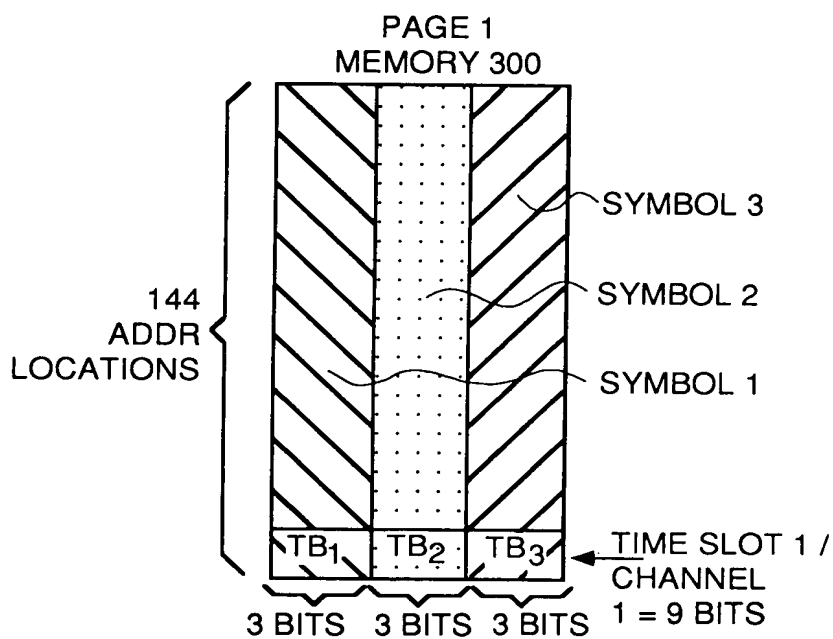
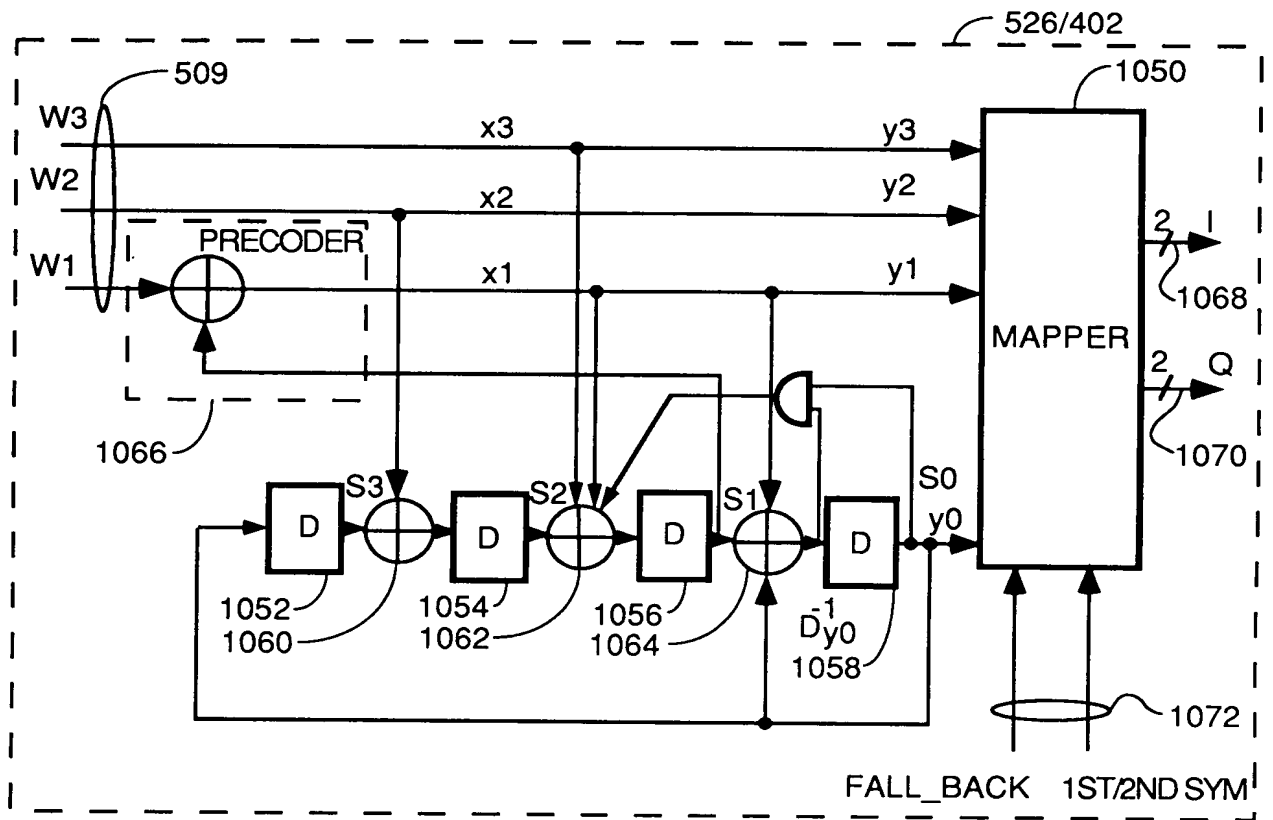


FIG. 16



PREFERRED TRELLIS ENCODER
FIG. 17

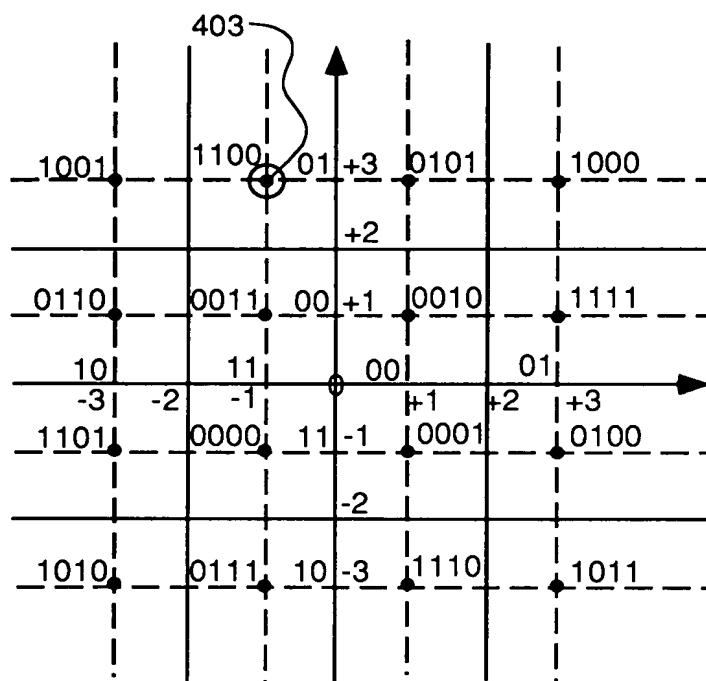


FIG. 18

0000	111	111	
0001	001	111	= 1 - j
0010	001	001	= 1 + j
0011	111	001	= -1 + j
0100	011	111	= 3 - j
0101	001	011	= 1 + 3*j
0110	101	001	= -3 + j
0111	111	101	= -1 - 3*j
1000	011	011	= +3 + 3*j
1001	101	011	= -3 + 3*j
1010	101	101	= -3 - 3*j
1011	011	101	= 3 - 3*j
1100	111	011	= -1 + 3*j
1101	101	111	= -3 - j
1110	001	101	= 1 - 3*j
1111	011	001	= 3 + j

FIG. 19

$$\begin{array}{c} \text{INFORMATION} \\ \text{VECTOR [B]} \\ \text{FOR EACH} \\ \text{SYMBOL} \end{array} \quad \begin{array}{c} 483 \\ 481 \end{array} \begin{bmatrix} 0 & 1 & 1 & 0 \\ 1 & 1 & 1 & 1 \\ 1 & 1 & 0 & 1 \\ 0 & 1 & 0 & 0 \\ \vdots & & & \end{bmatrix} \times \begin{array}{c} \text{ORTHOGONAL} \\ \text{CODE MATRIX} \end{array} \begin{bmatrix} C_{1,1} & C_{1,2} & \cdots & C_{1,144} \\ C_{2,1} & C_{2,2} & \cdots & C_{2,144} \\ \vdots & \vdots & & \vdots \end{bmatrix}$$

FIG. 20A

$$\begin{array}{c} \text{REAL} \\ \text{PART OF} \\ \text{INFO} \\ \text{VECTOR} \\ \text{[b]} \text{ FOR} \\ \text{FIRST} \\ \text{SYMBOL} \end{array} \quad \begin{array}{c} 405 \end{array} \begin{bmatrix} +3 \\ -1 \\ -1 \\ +3 \end{bmatrix} \cdot \begin{array}{c} 407 \end{array} \begin{bmatrix} 1 & 1 & 1 & 1 \\ -1 & -1 & 1 & 1 \\ -1 & 1 & -1 & 1 \\ -1 & 1 & 1 & -1 \end{bmatrix} = \begin{array}{c} \text{REAL} \\ \text{PART OF} \\ \text{RESULT} \\ \text{VECTOR} \end{array} \quad \begin{array}{c} 409 \end{array} \begin{bmatrix} 4 \\ 0 \\ 0 \\ -8 \end{bmatrix}$$

$$[b_{\text{REAL}}] \times [\text{CODE MATRIX}] = [R_{\text{REAL}}] = \text{"CHIPS OUT" ARRAY-REAL}$$

FIG. 20B

MAPPING FOR FALL-BACK MODE - LSB'S

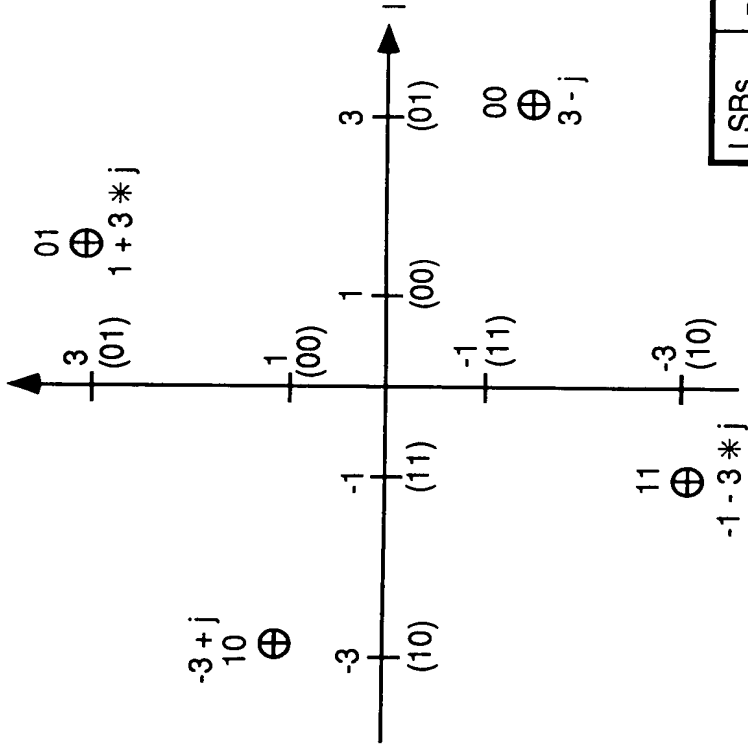


FIG. 21

MSBs y3 y2	1+jQ WHEN LSB=00	1+jQ WHEN LSB=01	1+jQ WHEN LSB=10	1+jQ WHEN LSB=11
00	3-j	1+j3	-3+j	-1-j3
01	1+j3	-3+j	-1-j3	3-j
10	-3+j	-1-j3	3-j	1+j3
11	-1-j3	3-j	1+j3	-3+j

LSBs y1 y0	PHASE	1+jQ
00	0	3-j
01	90	1+j3
10	180	-3+j
11	-90	-1-j3

LSB & MSB FALLBACK MODE MAPPINGS

FIG. 22

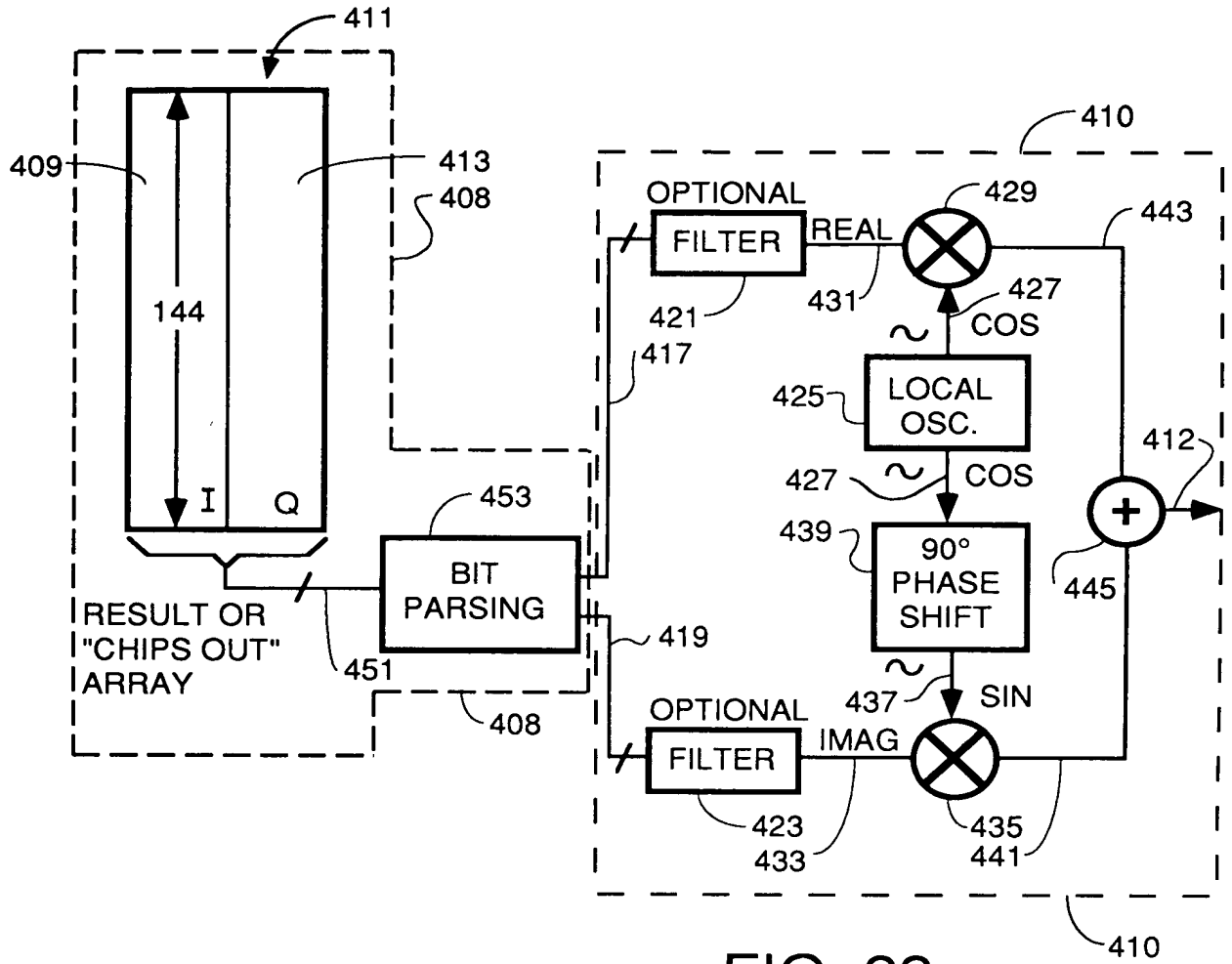


FIG. 23

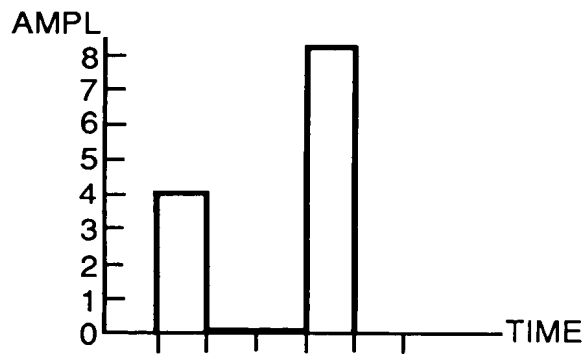


FIG. 24

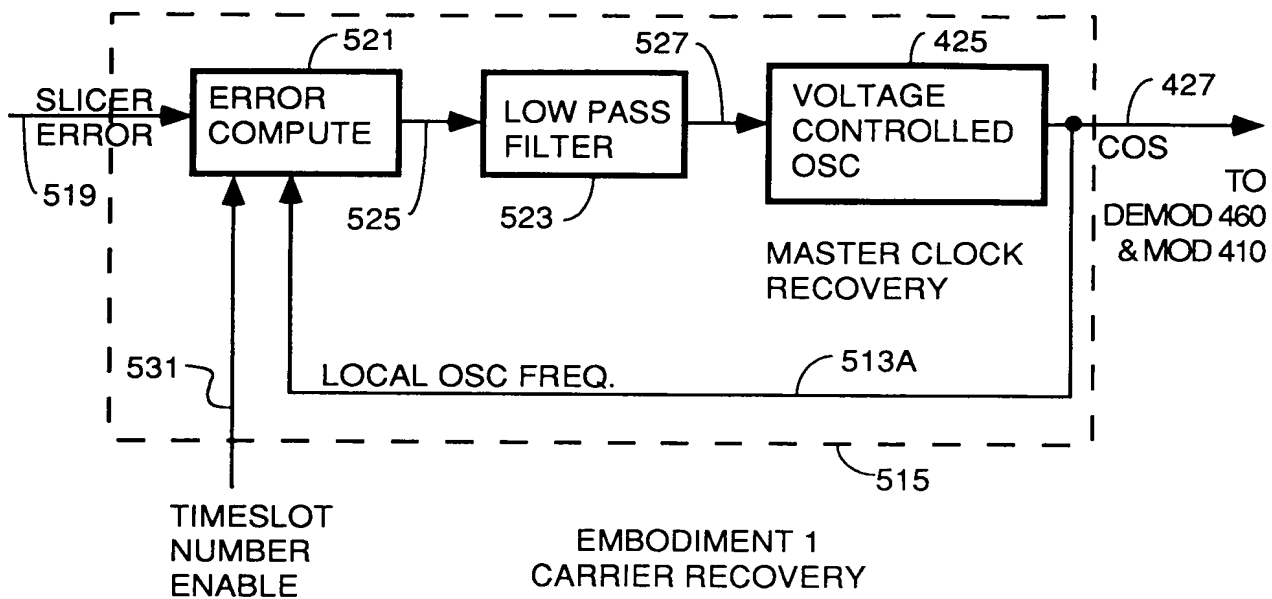


FIG. 25

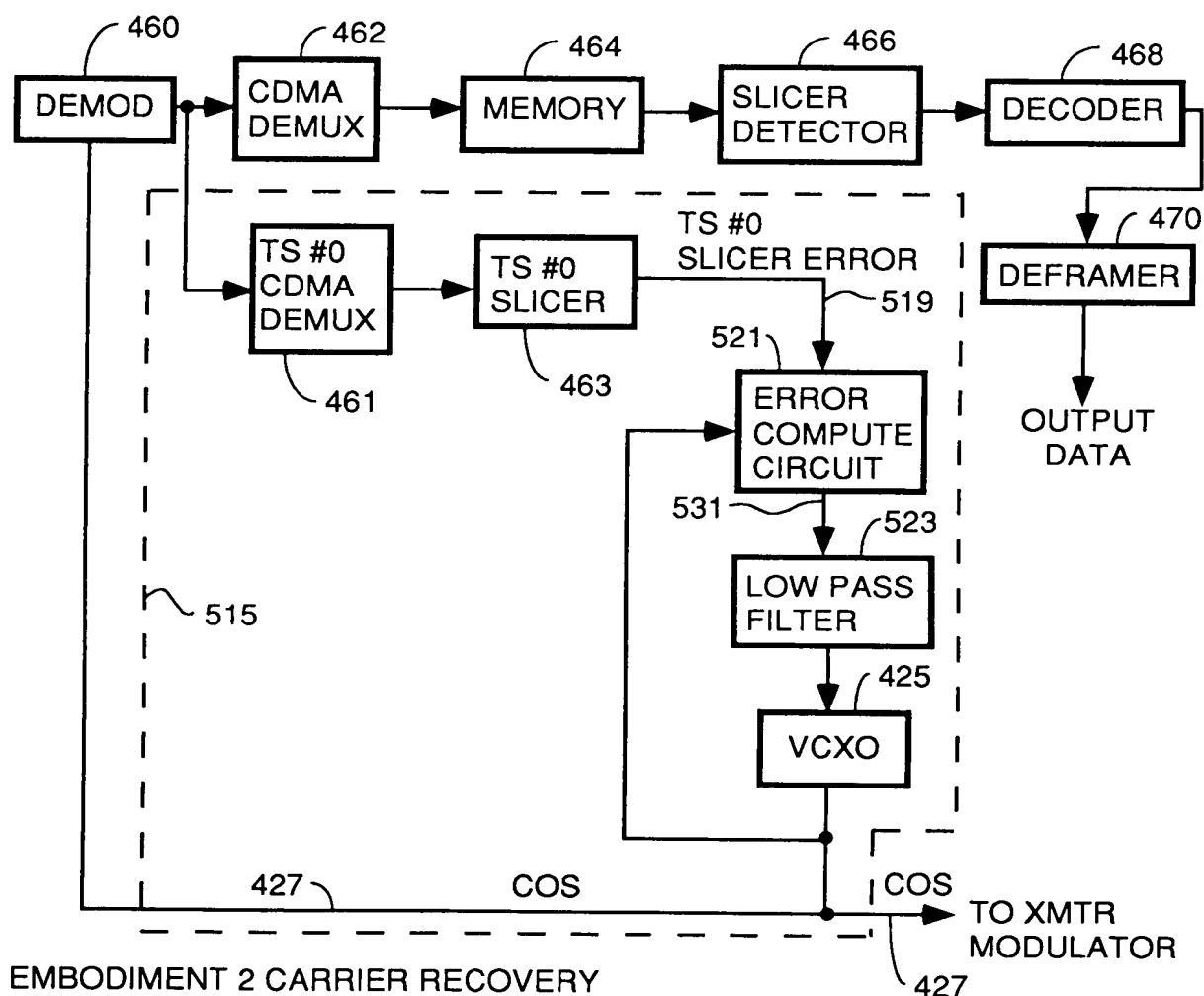


FIG. 26

09759774-04401

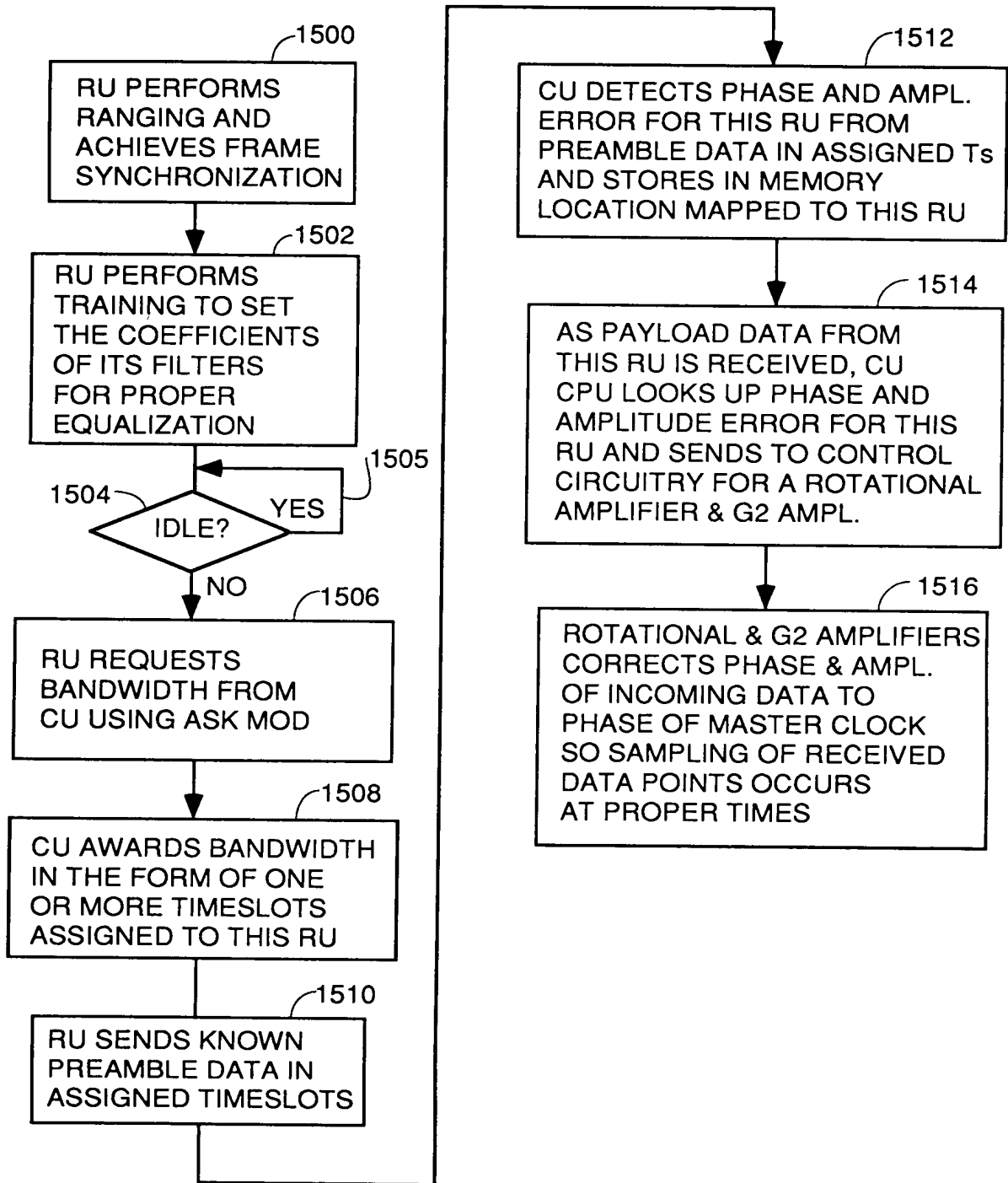
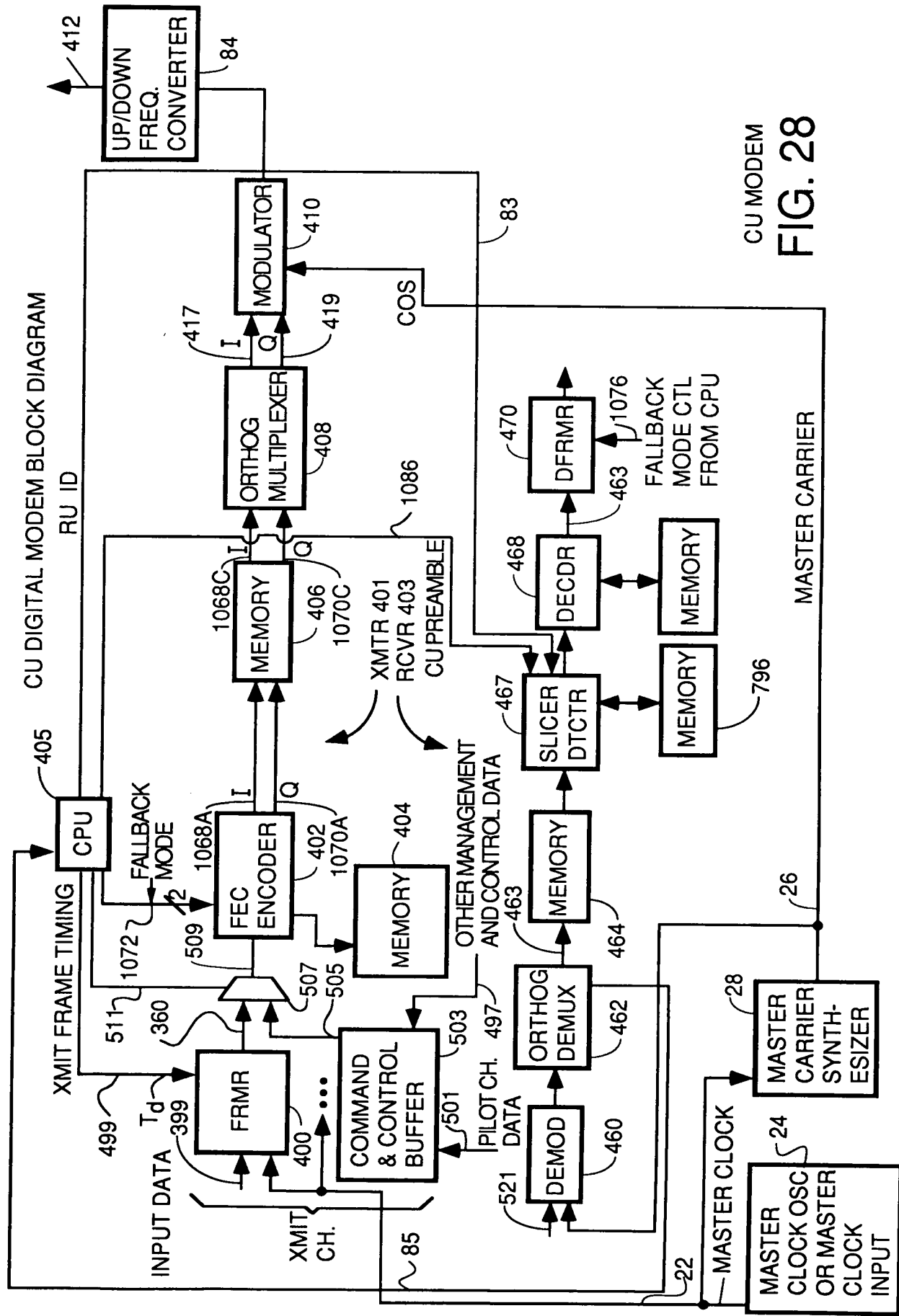


FIG. 27



CU MODEM
FIG. 28

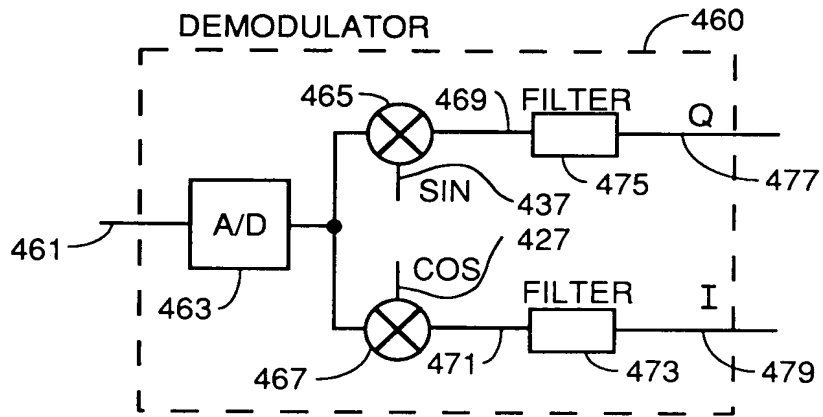


FIG. 29

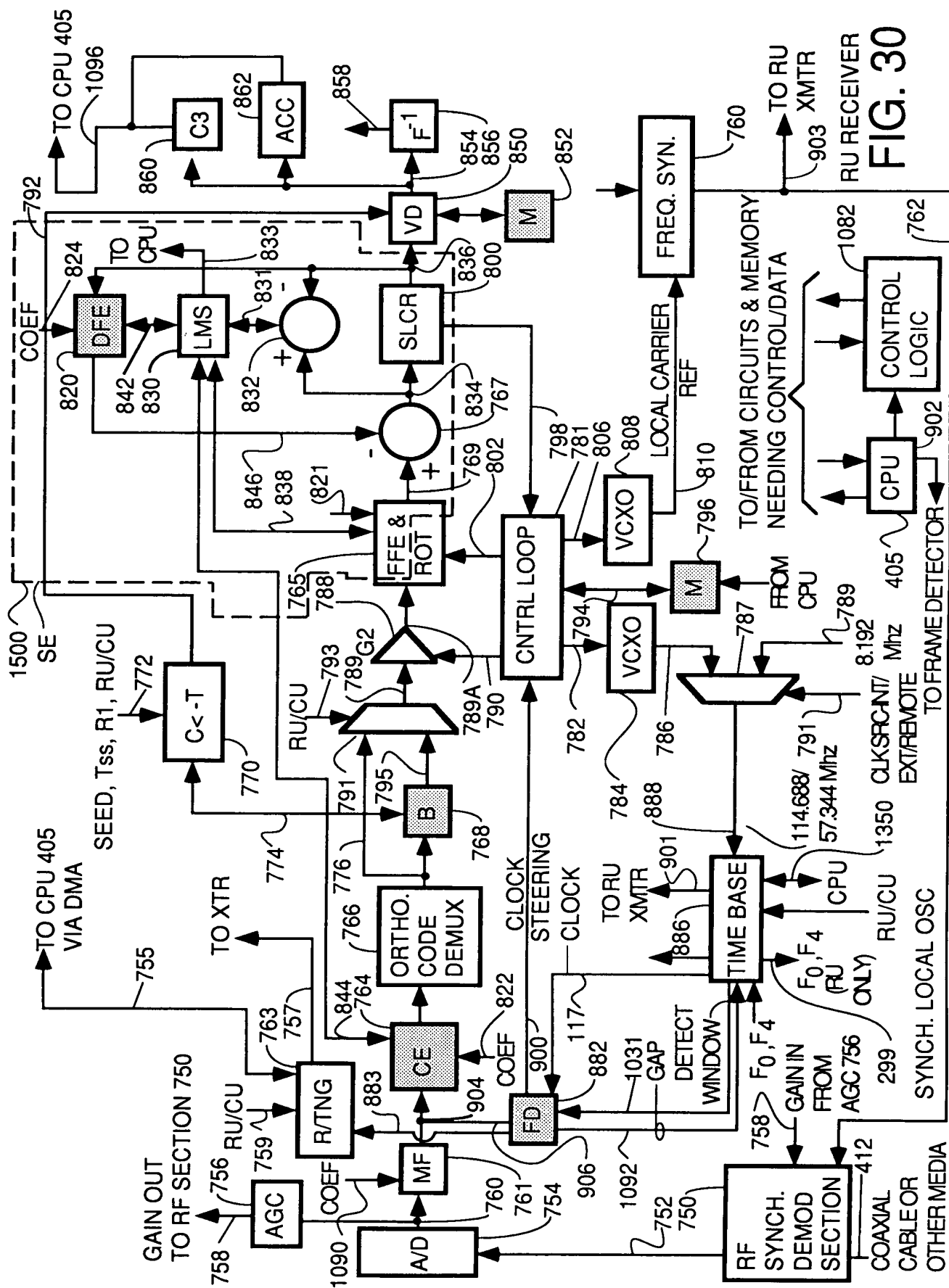
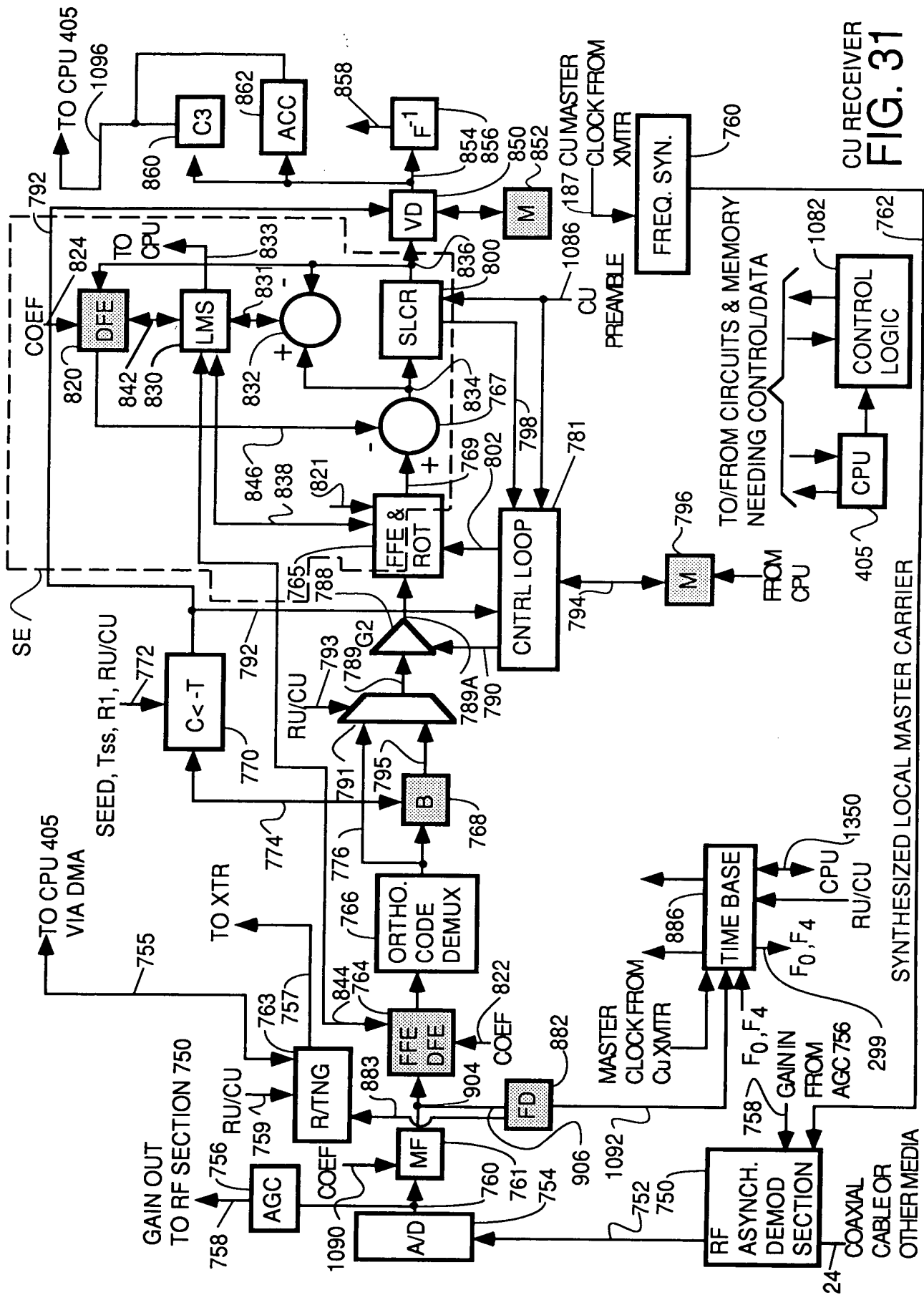
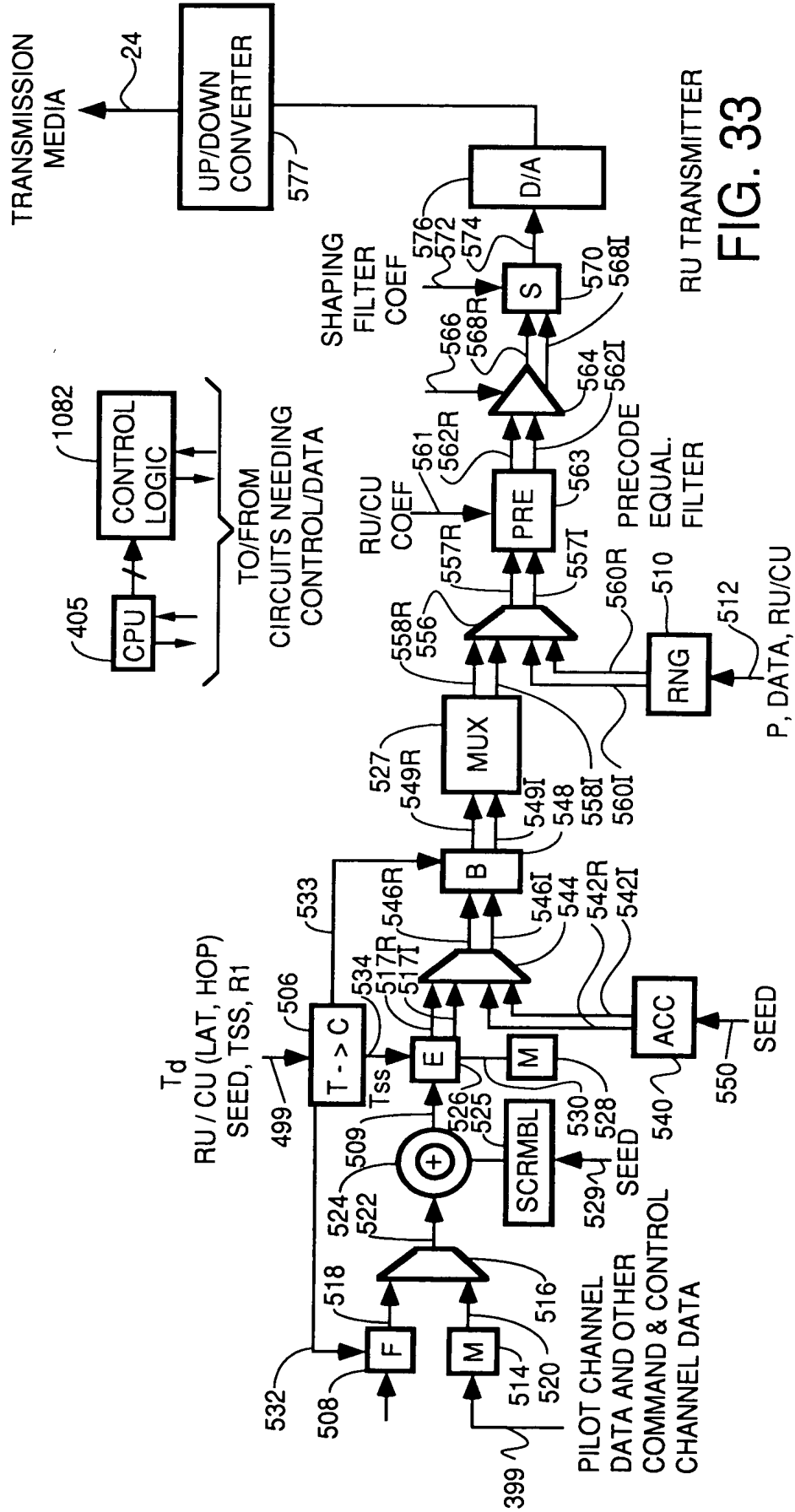


FIG. 30





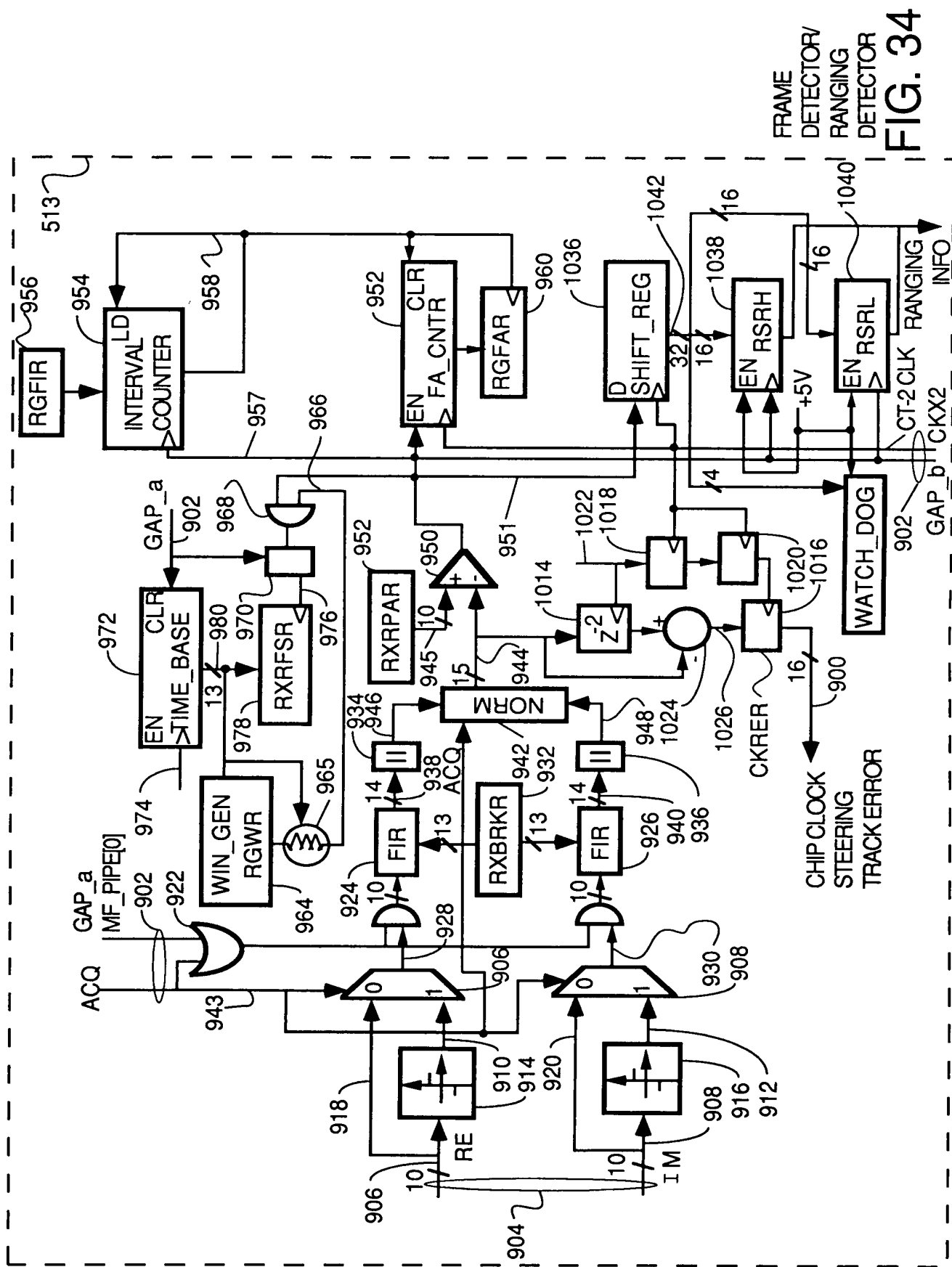


FIG. 34

FIG. 35

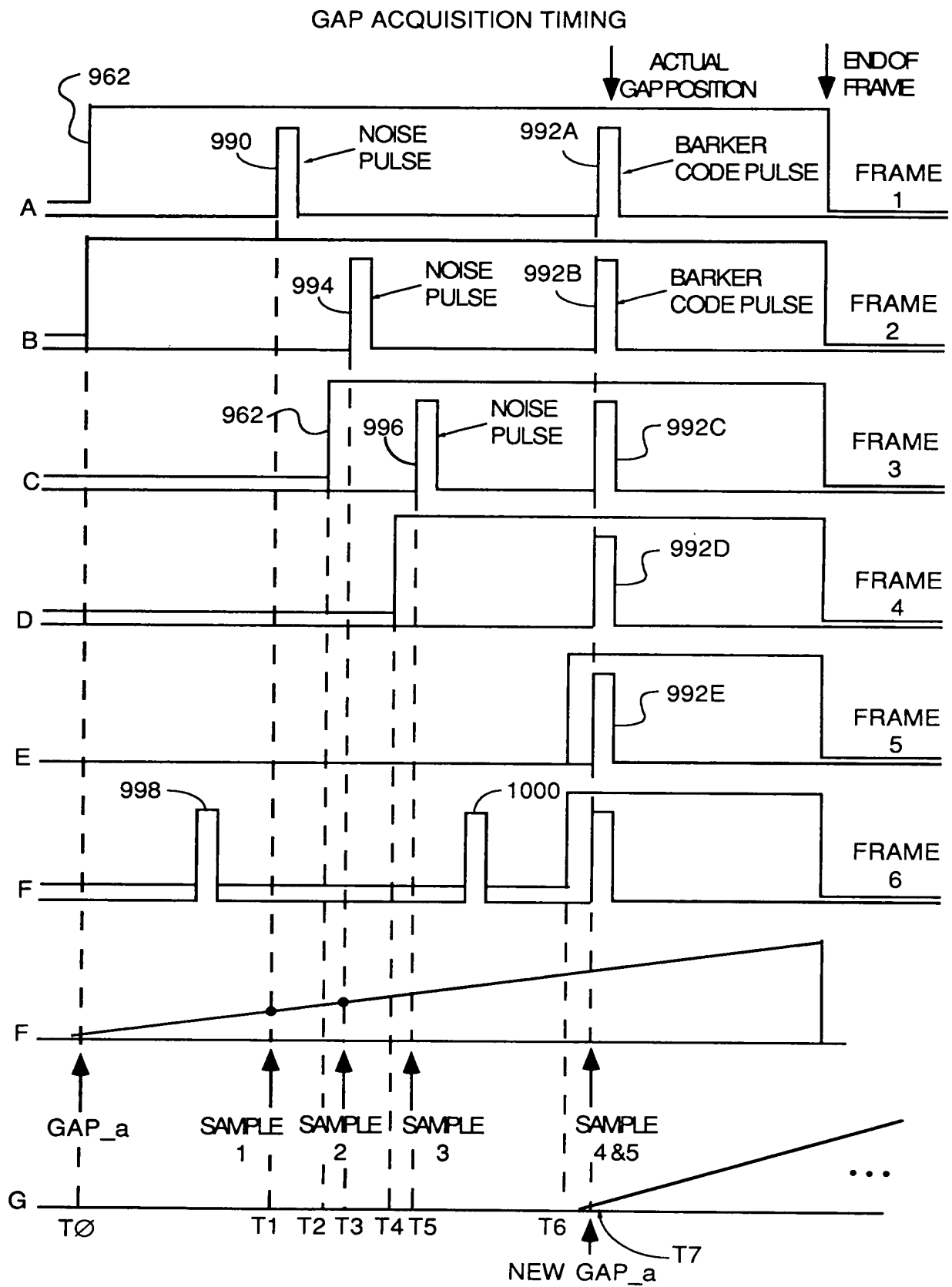


FIG. 35

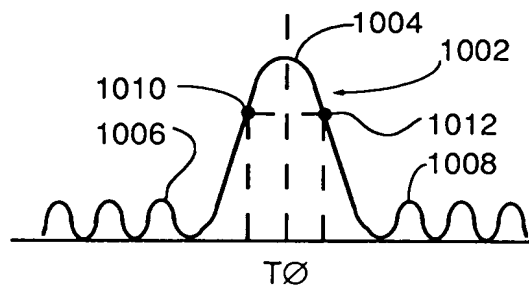


FIG. 36

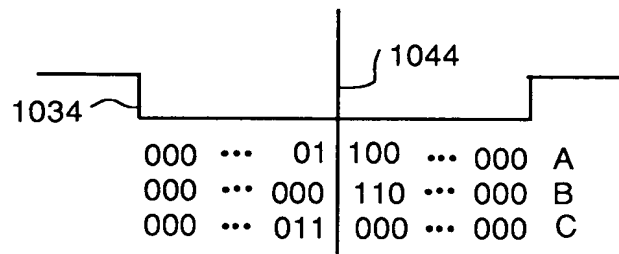


FIG. 37
FINE TUNING TO
CENTER BARKER CODE

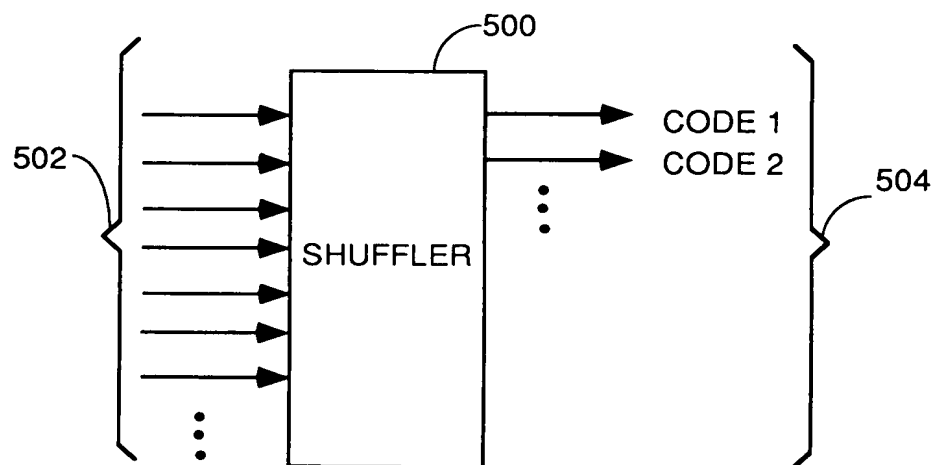


FIG. 38

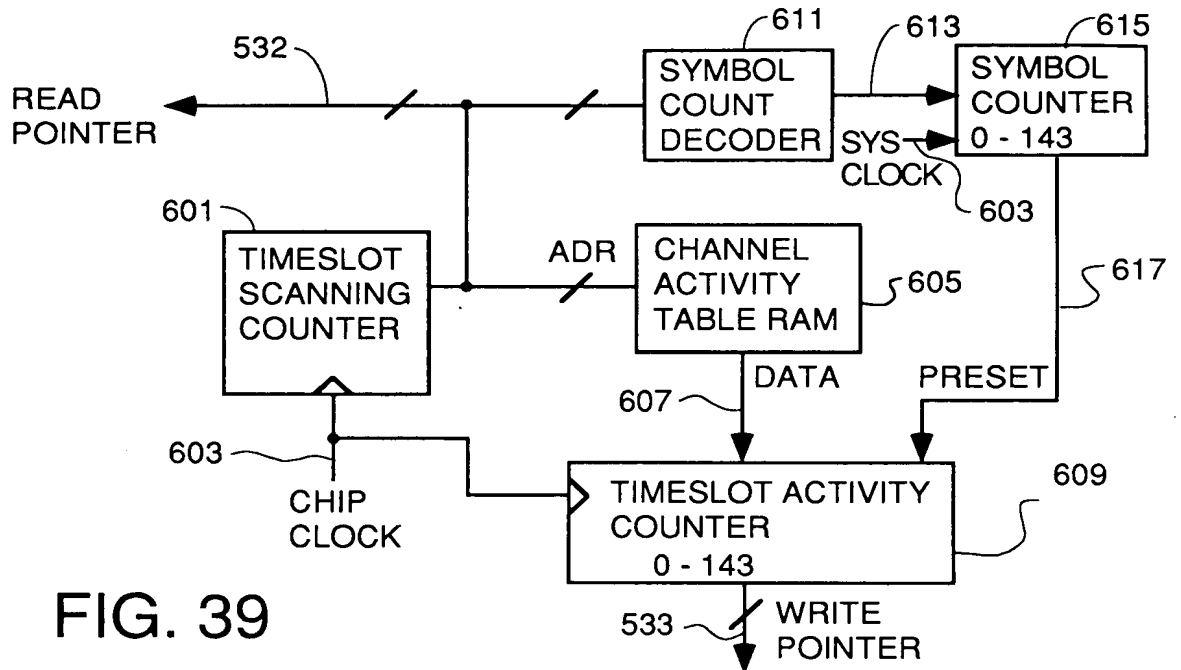


FIG. 39

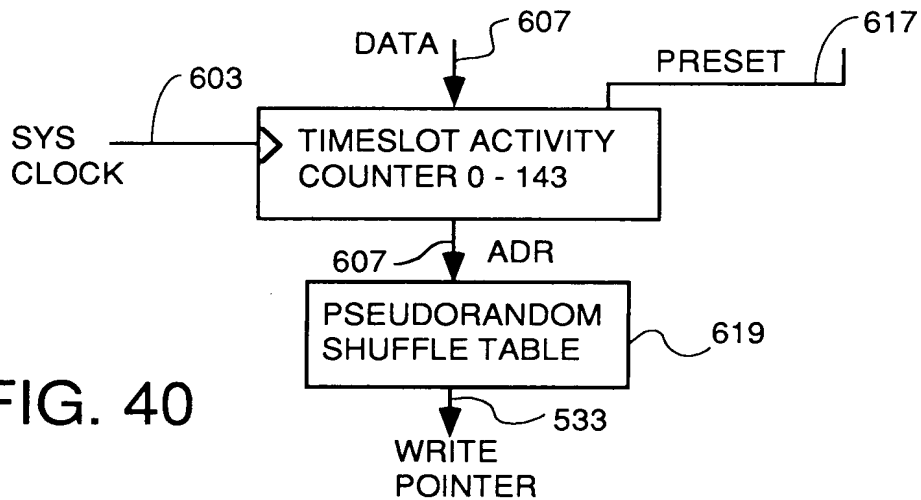


FIG. 40

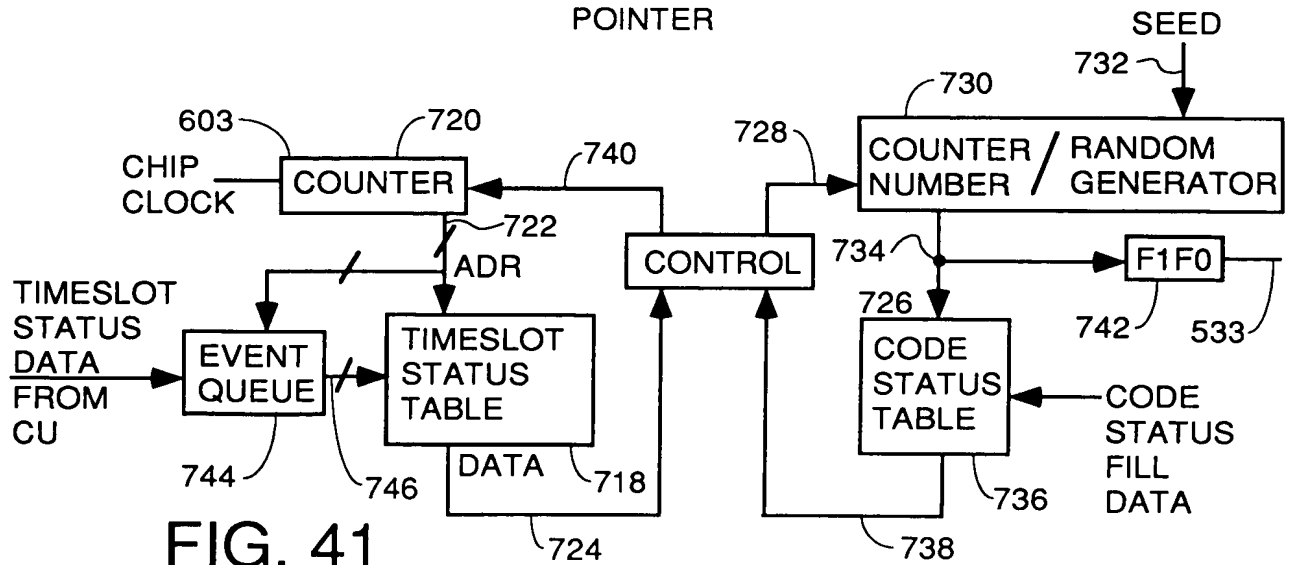


FIG. 41

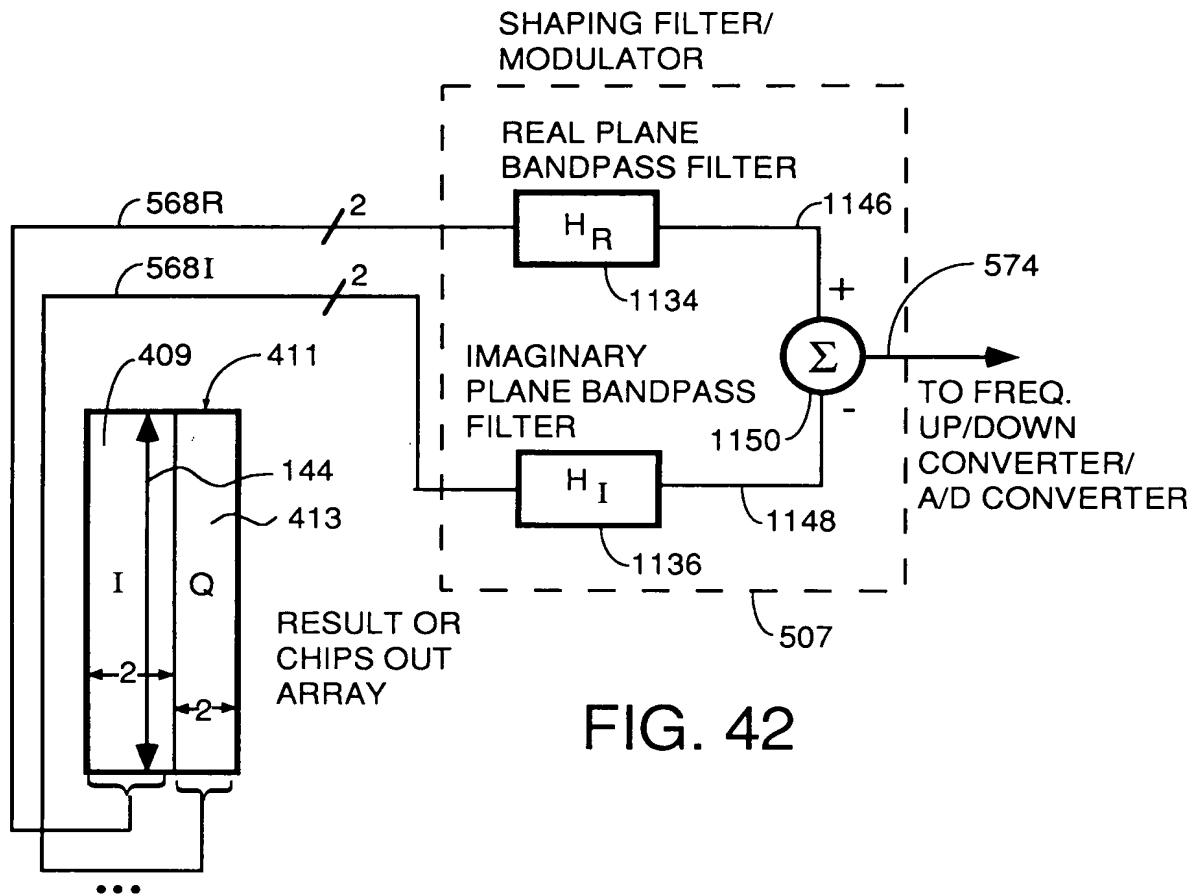


FIG. 42

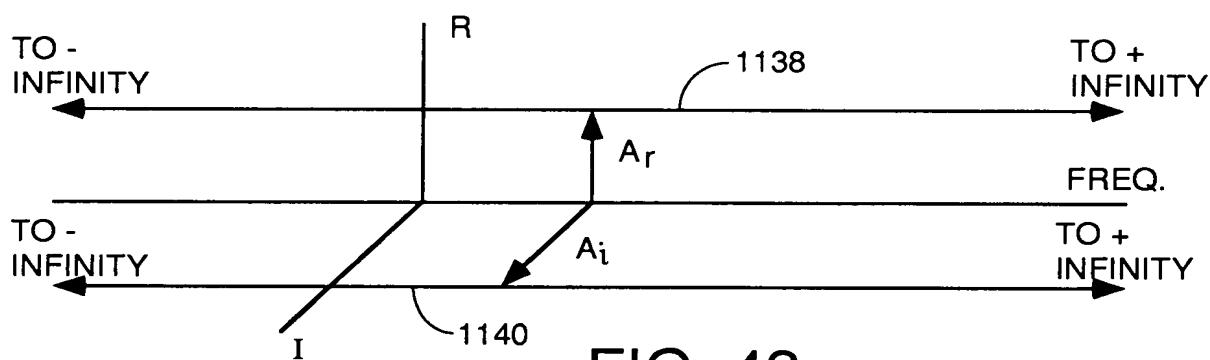


FIG. 43

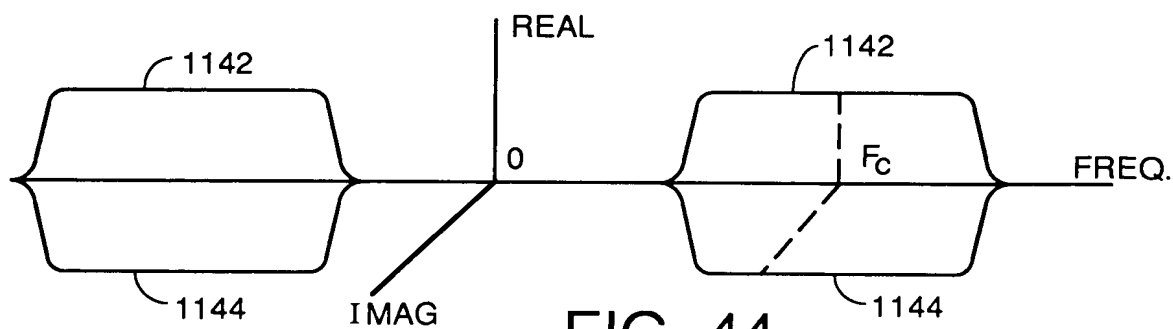
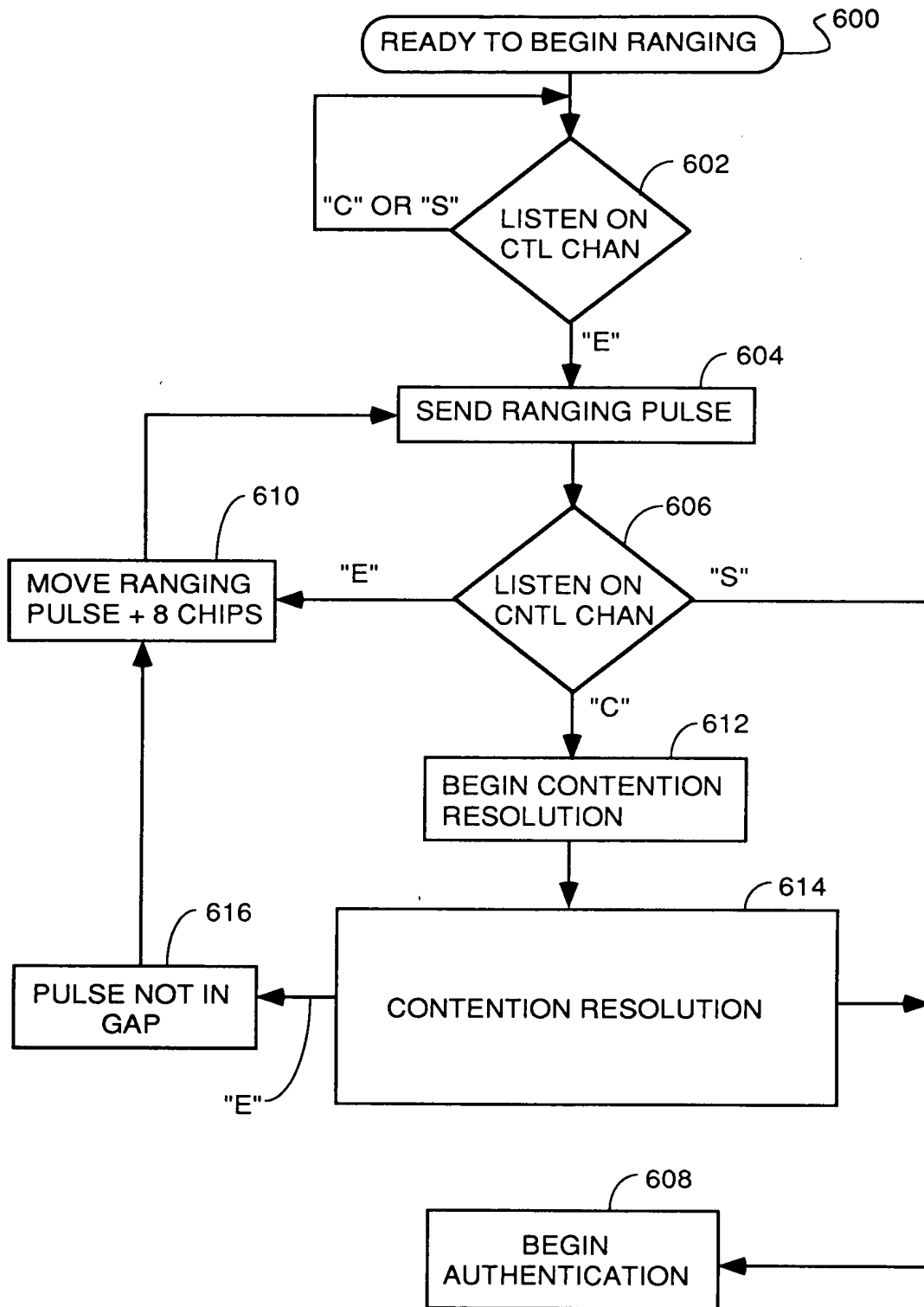


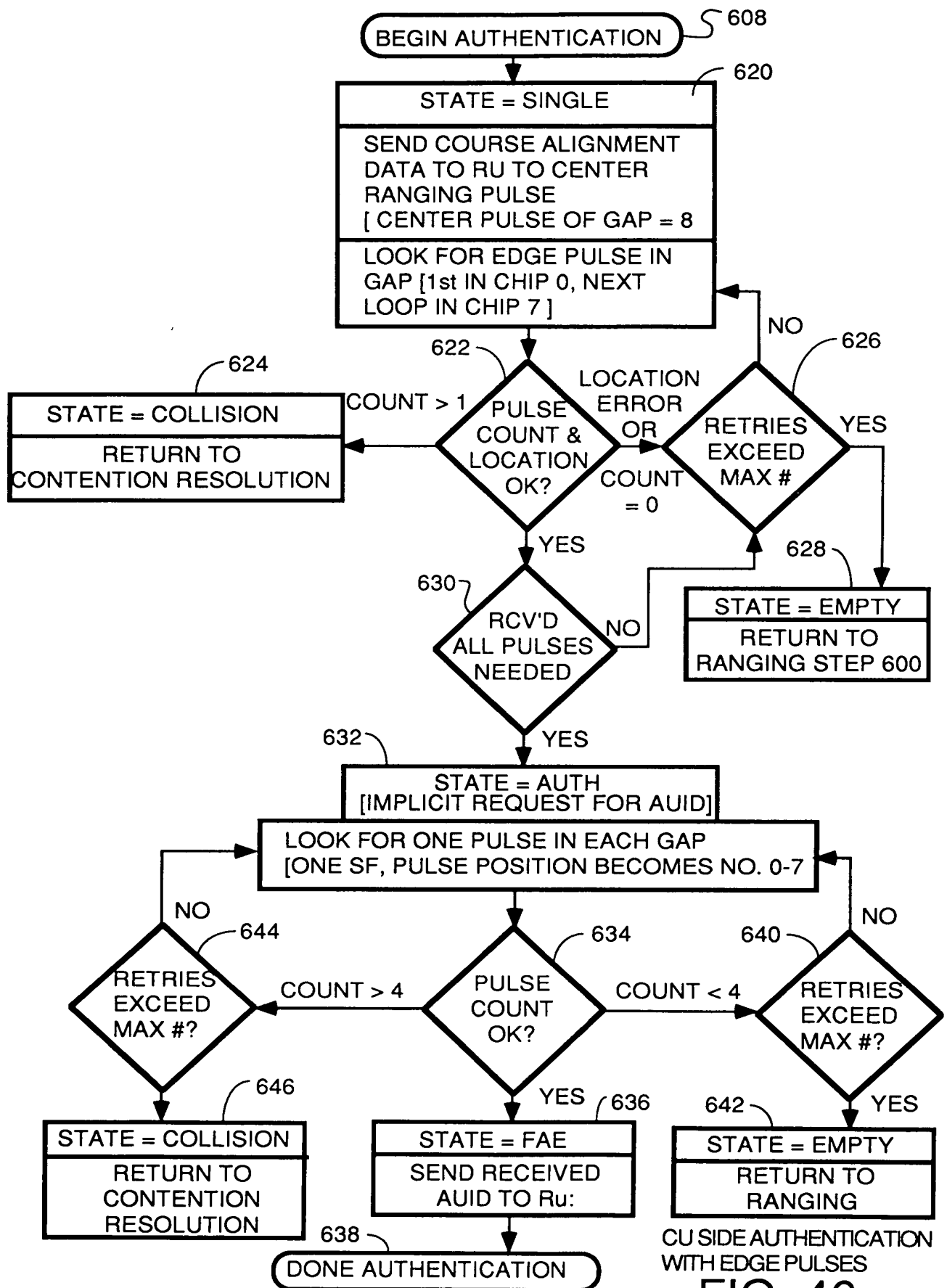
FIG. 44

0975974.041201
"02140" 4265250



RU RANGING
FIG. 45

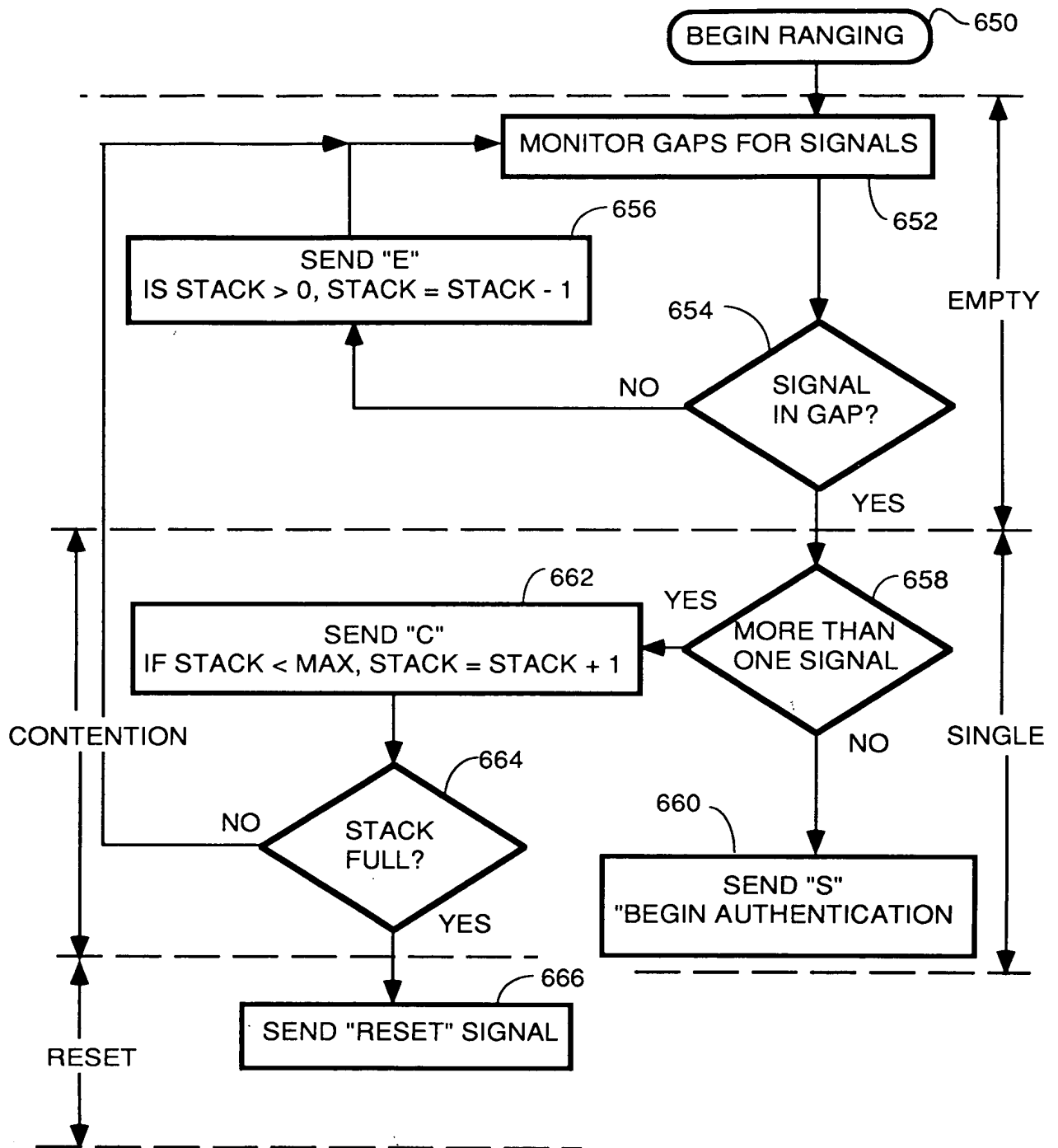
09759774-041201



CU SIDE AUTHENTICATION
WITH EDGE PULSES

FIG. 46

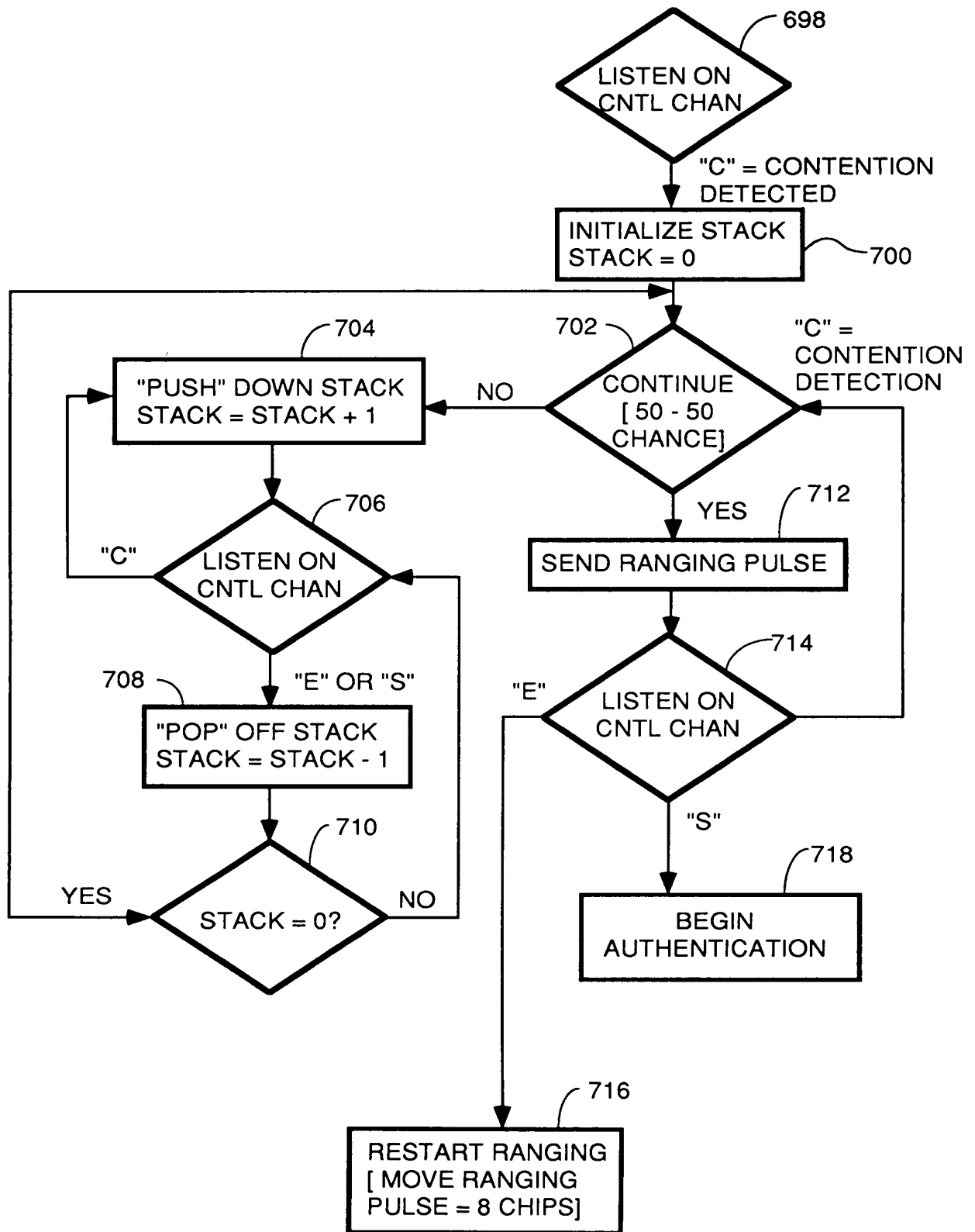
FIG. 47



CU RANGING AND CONTENTION RESOLUTION

FIG. 47

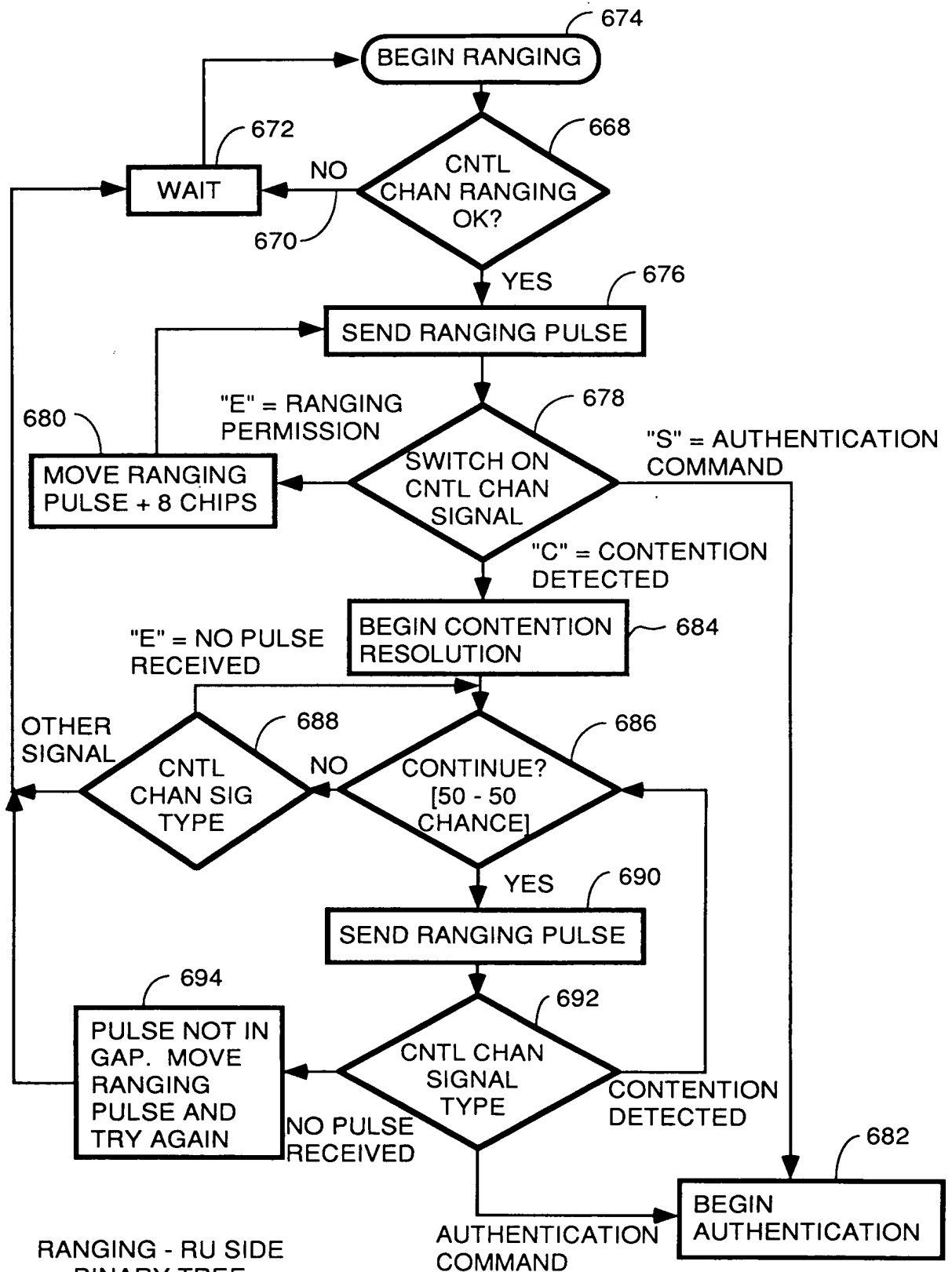
FIG. 48



CONTENTION RESOLUTION - RU
USING BINARY STACK

FIG. 48

FIG. 49



RANGING - RU SIDE
BINARY TREE
ALGORITHM

FIG. 49

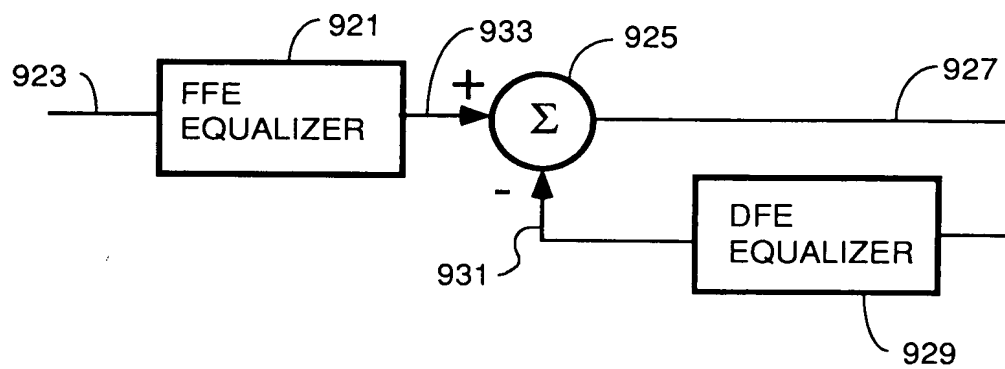


FIG. 50

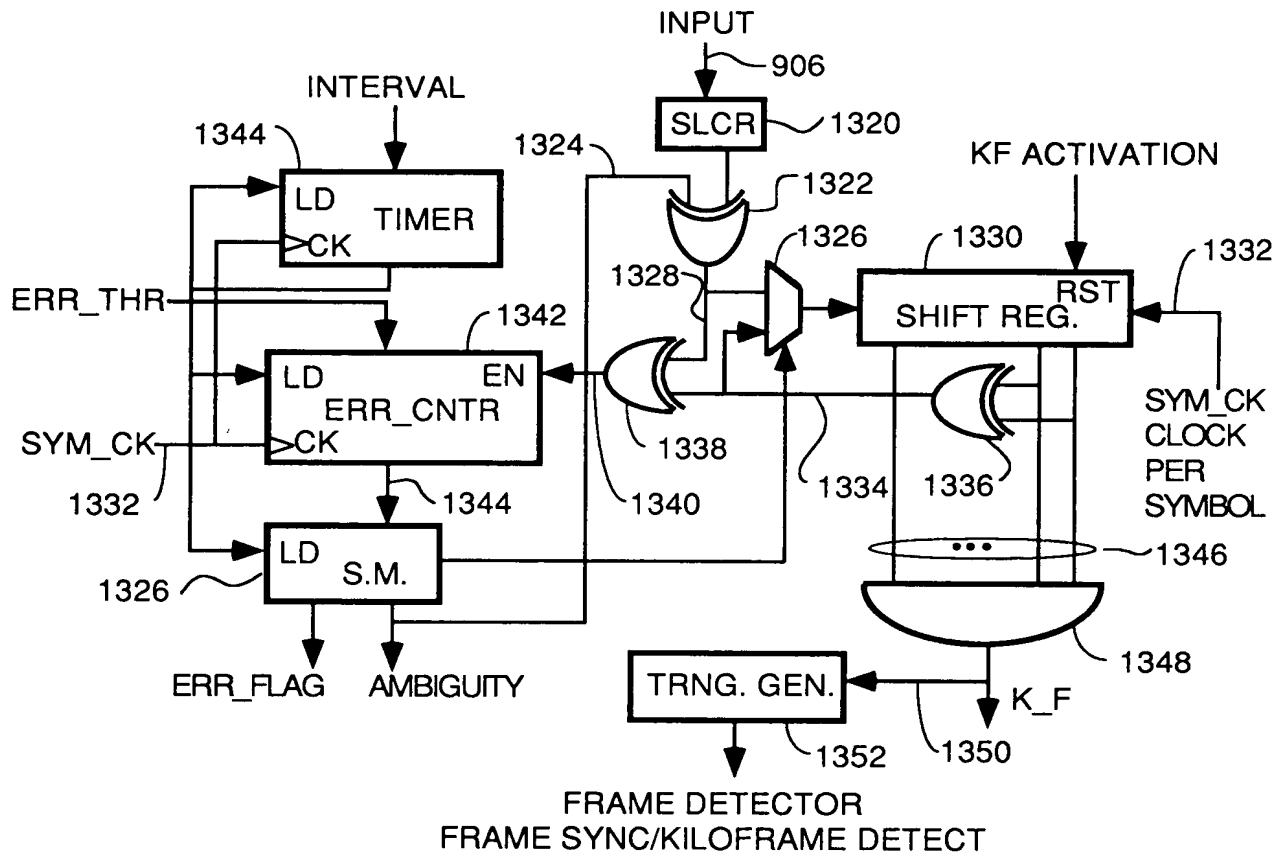
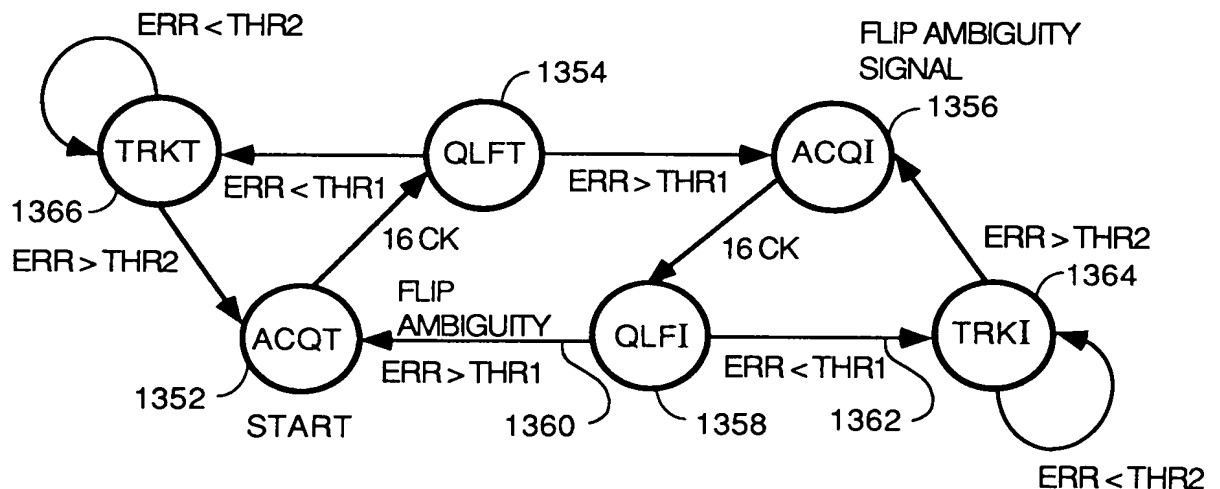


FIG. 51



STATE MACHINE
FIG. 52

PRECHANNEL EQUALIZATION TRAINING ALGORITHM

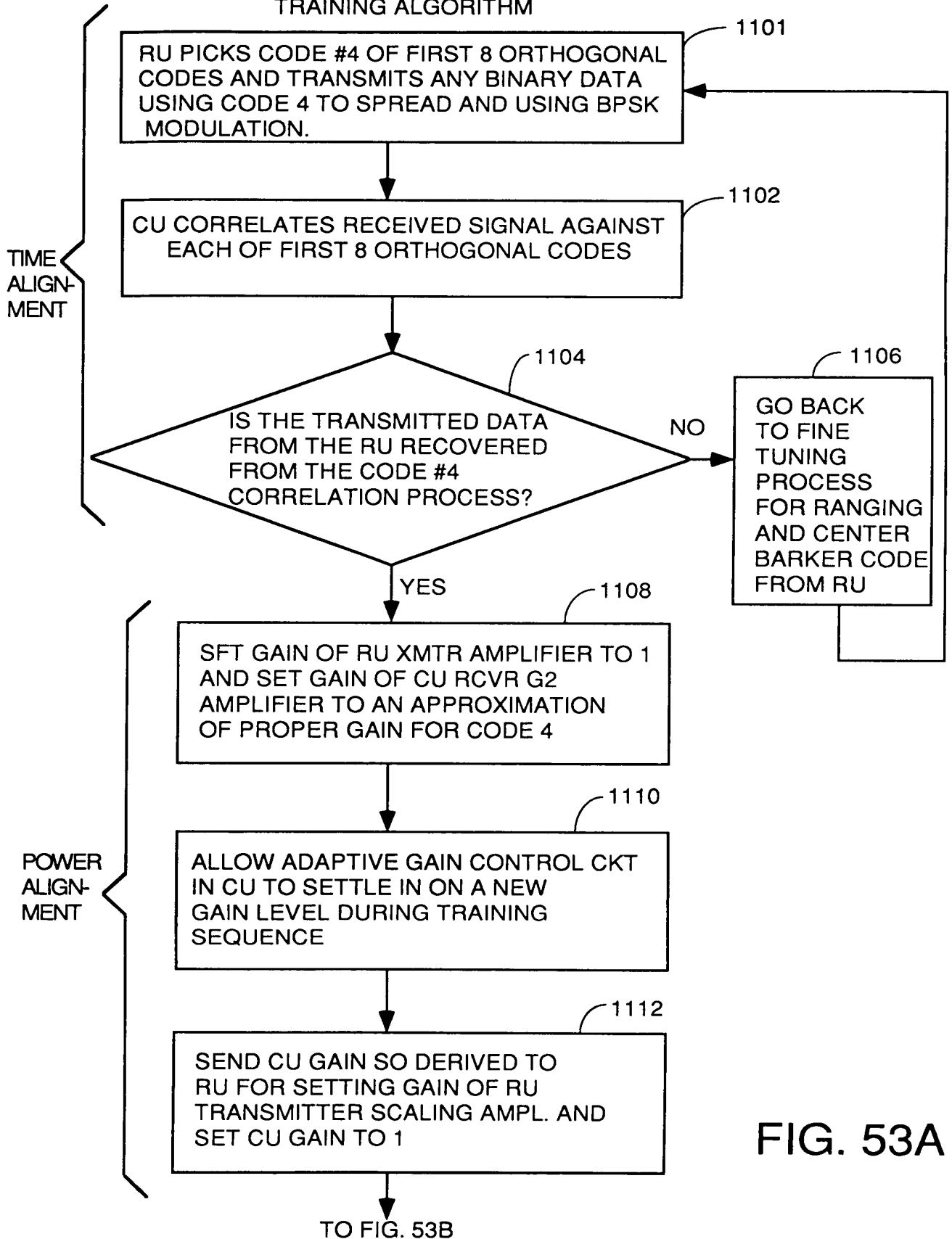


FIG. 53A

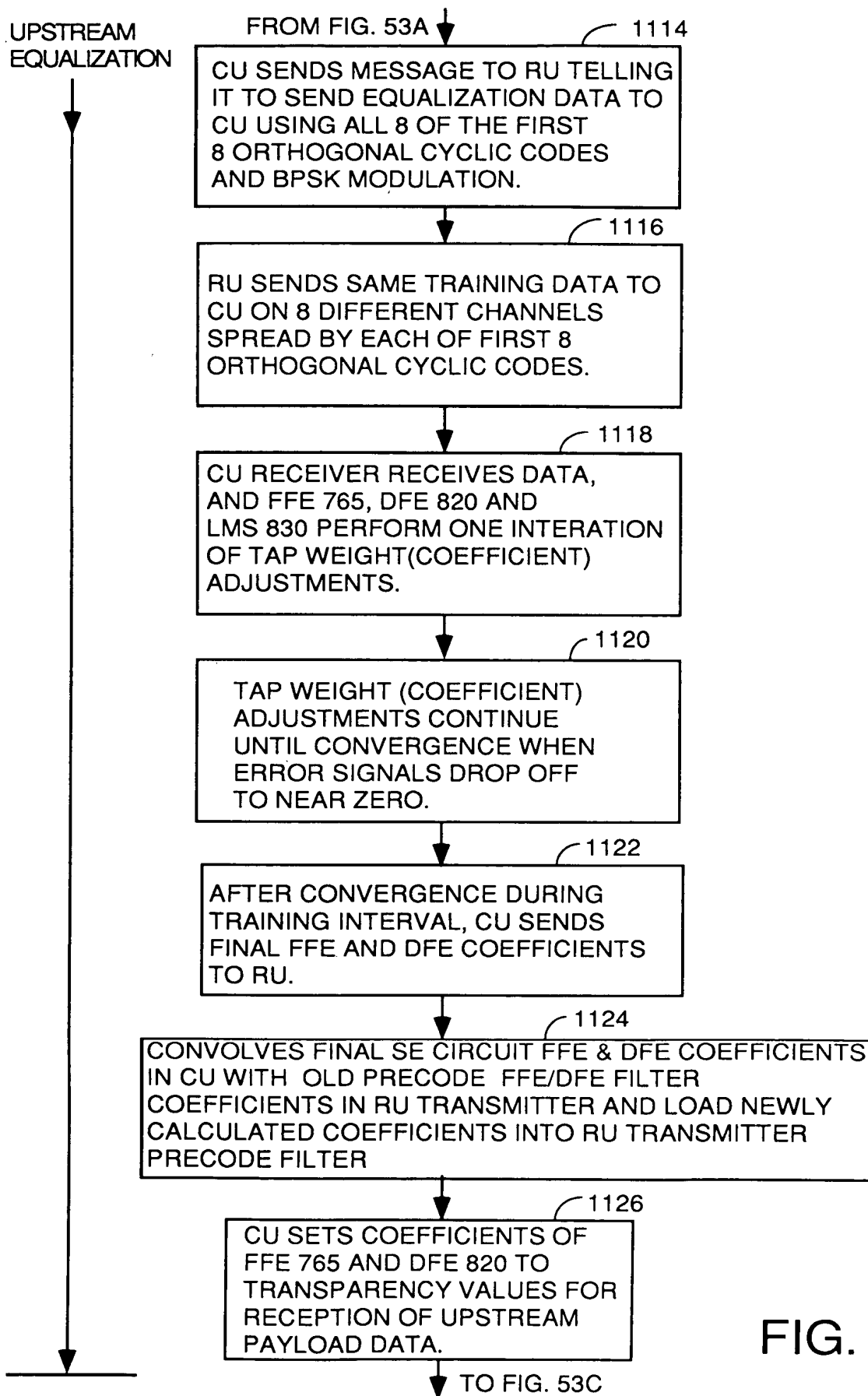


FIG. 53B

09759744.04260

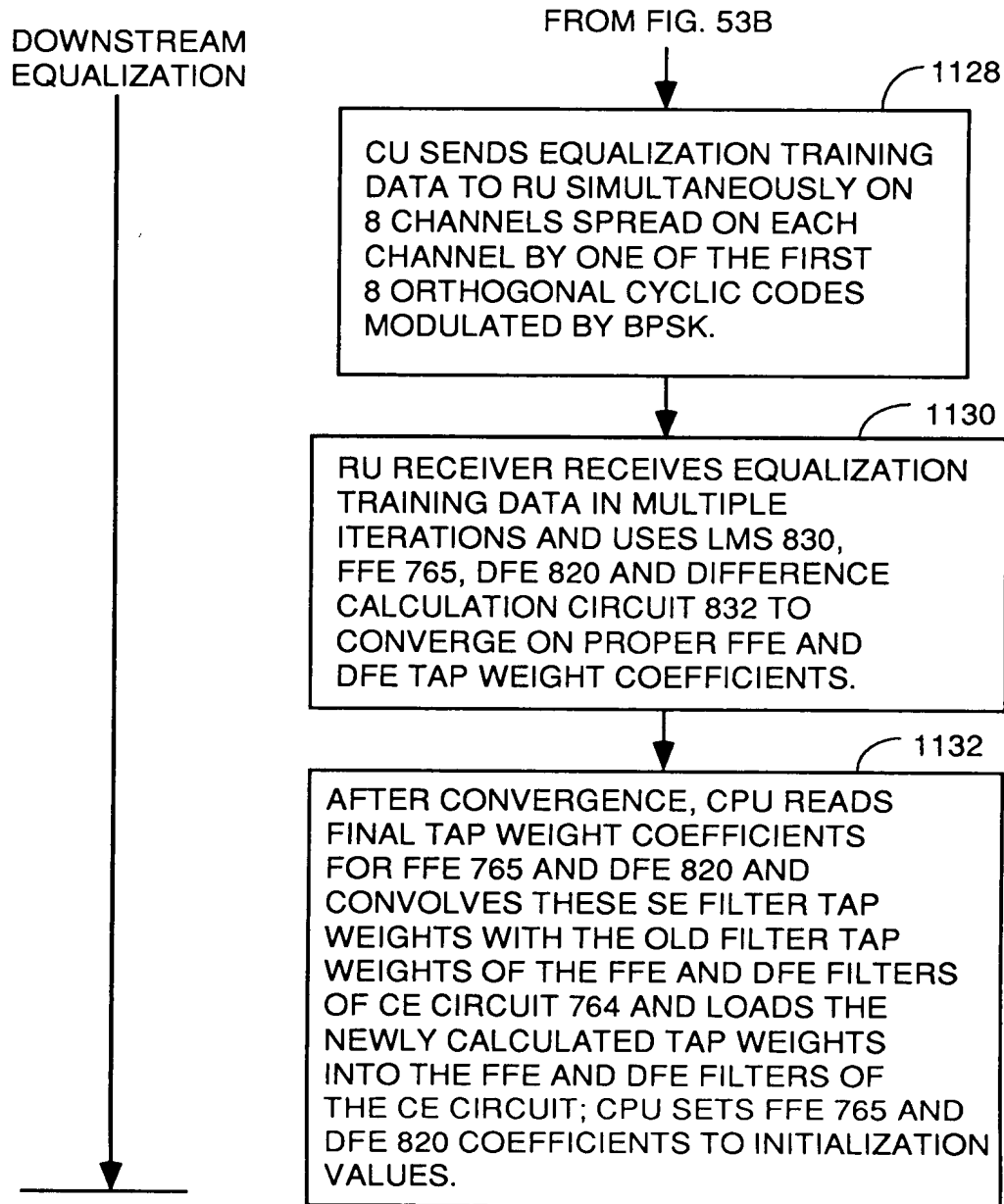


FIG. 53C

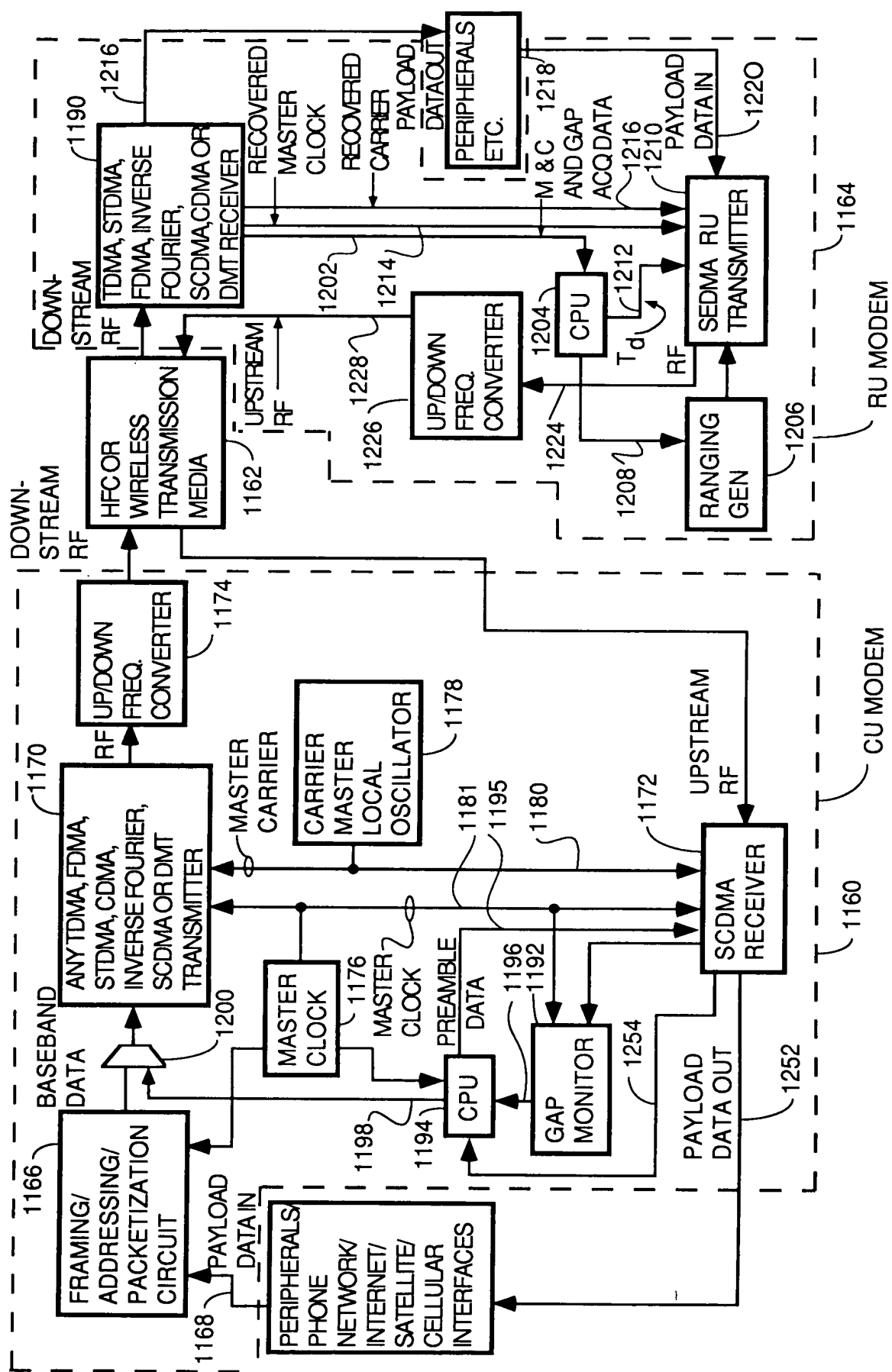
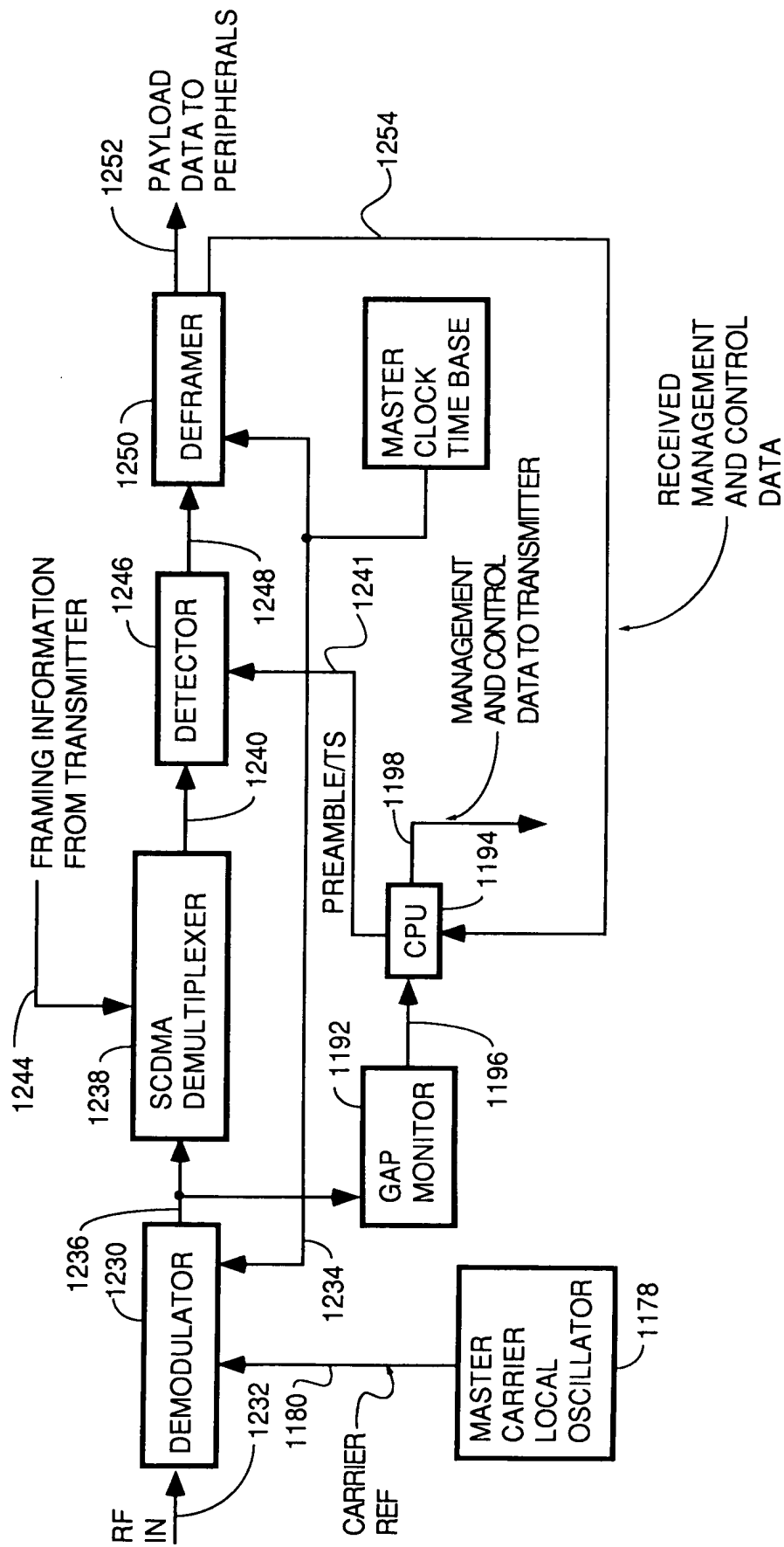


FIG. 54



SIMPLE CU SPREAD SPECTRUM RECEIVER

FIG. 55

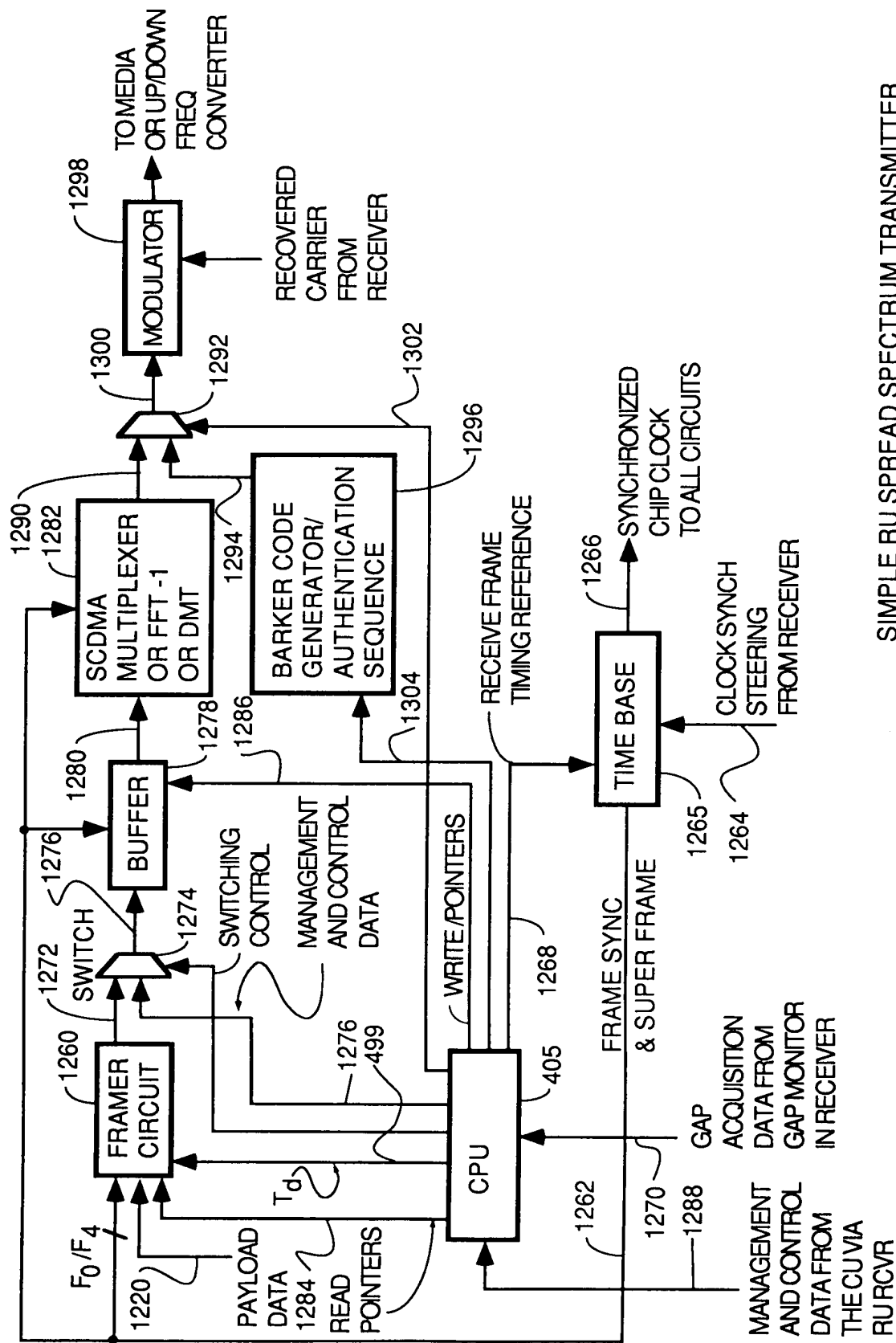
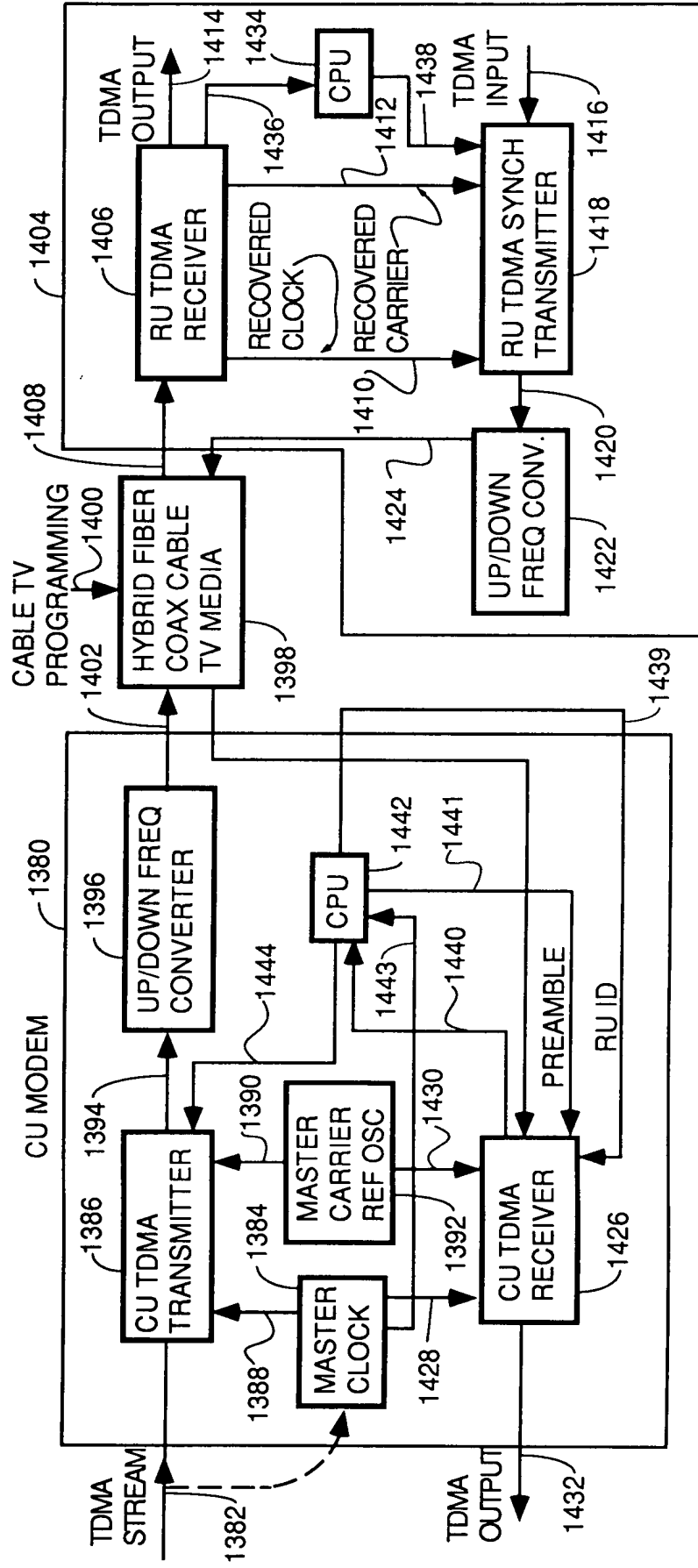


FIG. 56



SYNCHRONOUS TDMA SYSTEM

FIG. 57

0975974.041201
FIG. 58

OFFSET	1B ASIC		2A ASIC	
(CHIPS)	RGSRH	RGSRL	RGSRH	RGSRL
0	0x0000	0x8000	0x0001	0x0000
1/2	0x0000	0xC000	0x0001	0x8000
1	0x0000	0x4000	0x0000	0x8000
-1	0x0001	0x0000	0x0002	0x0000

FIG. 58

TRAINING ALGORITHM
SE FUNCTION

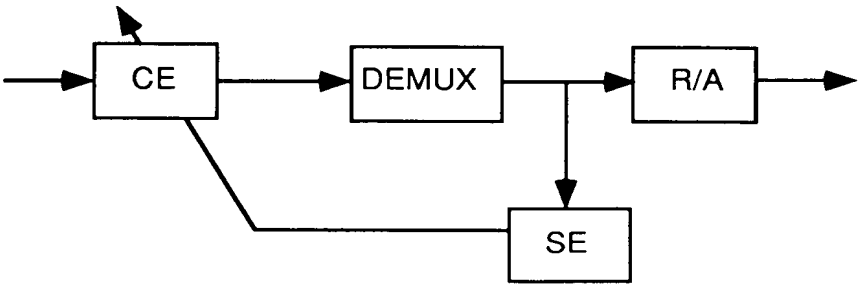
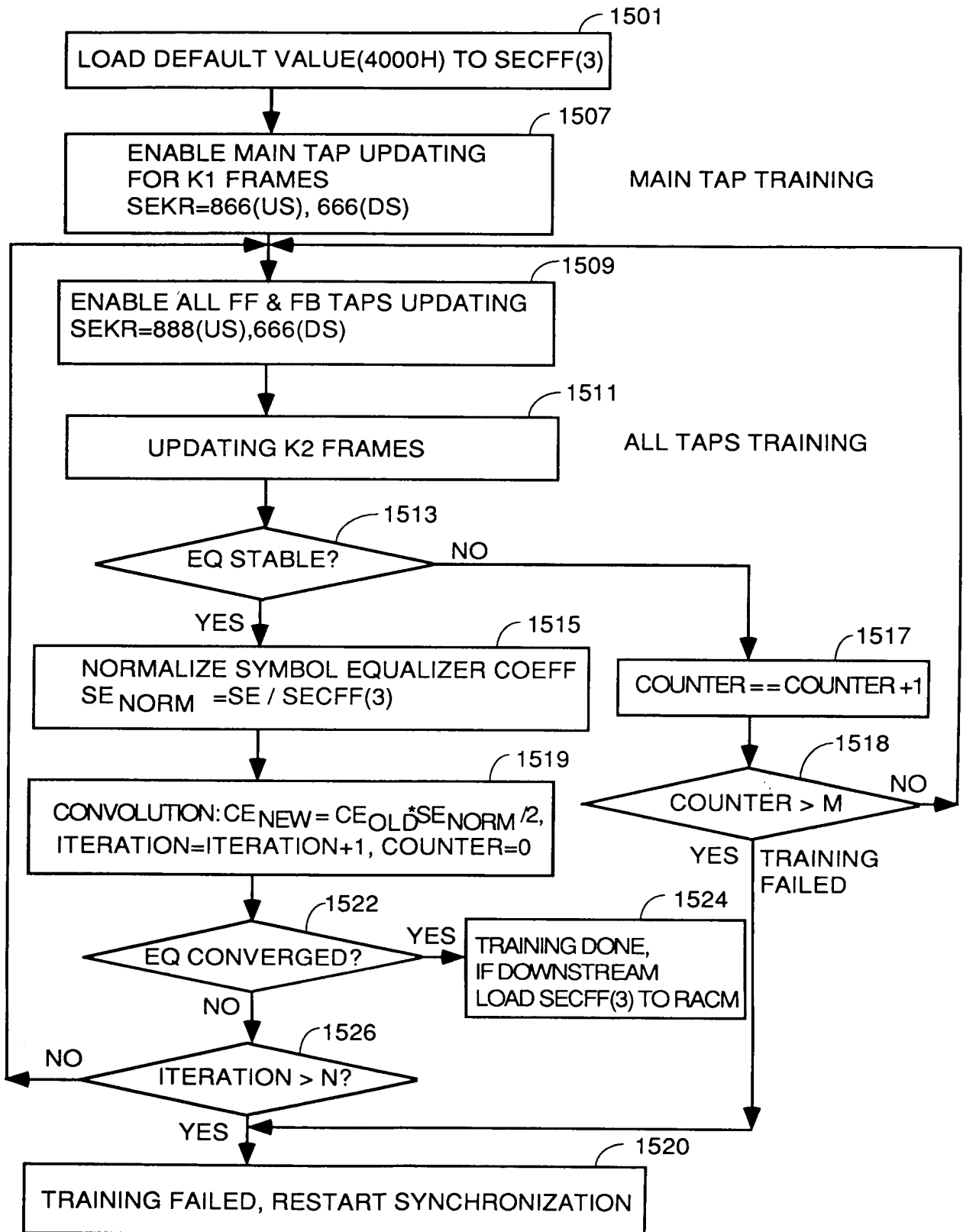


FIG. 59

INITIAL 2-STEP TRAINING ALGORITHM



2-STEP INITIAL EQUALIZATION TRAINING

FIG. 60

EQ STABILITY CHECK

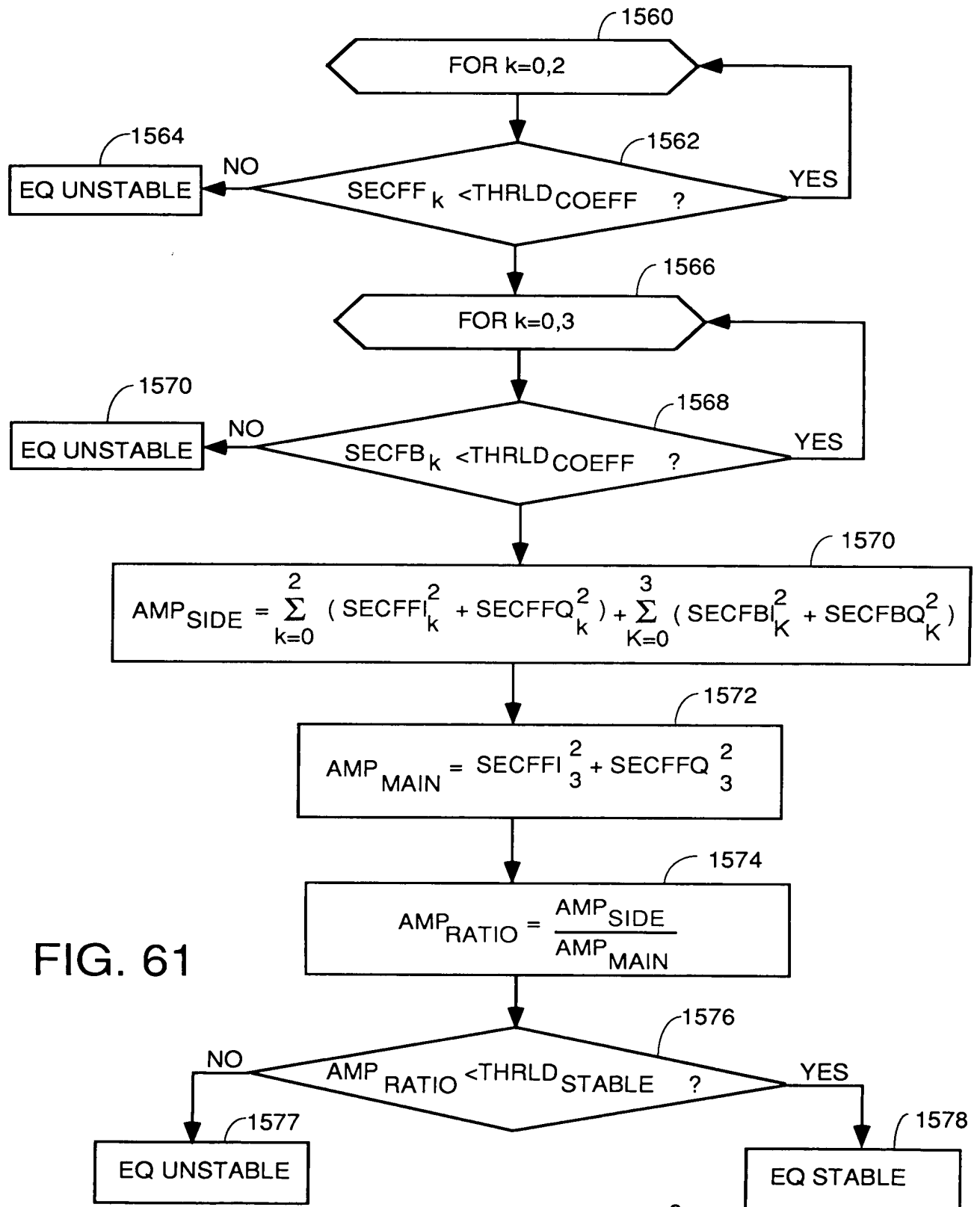


FIG. 61

NOTE: THRLD_COEFF = 7F00H

THRLD_STABLE = 10⁻³

095974-0434

PERIODIC 2-STEP TRAINING ALGORITHM

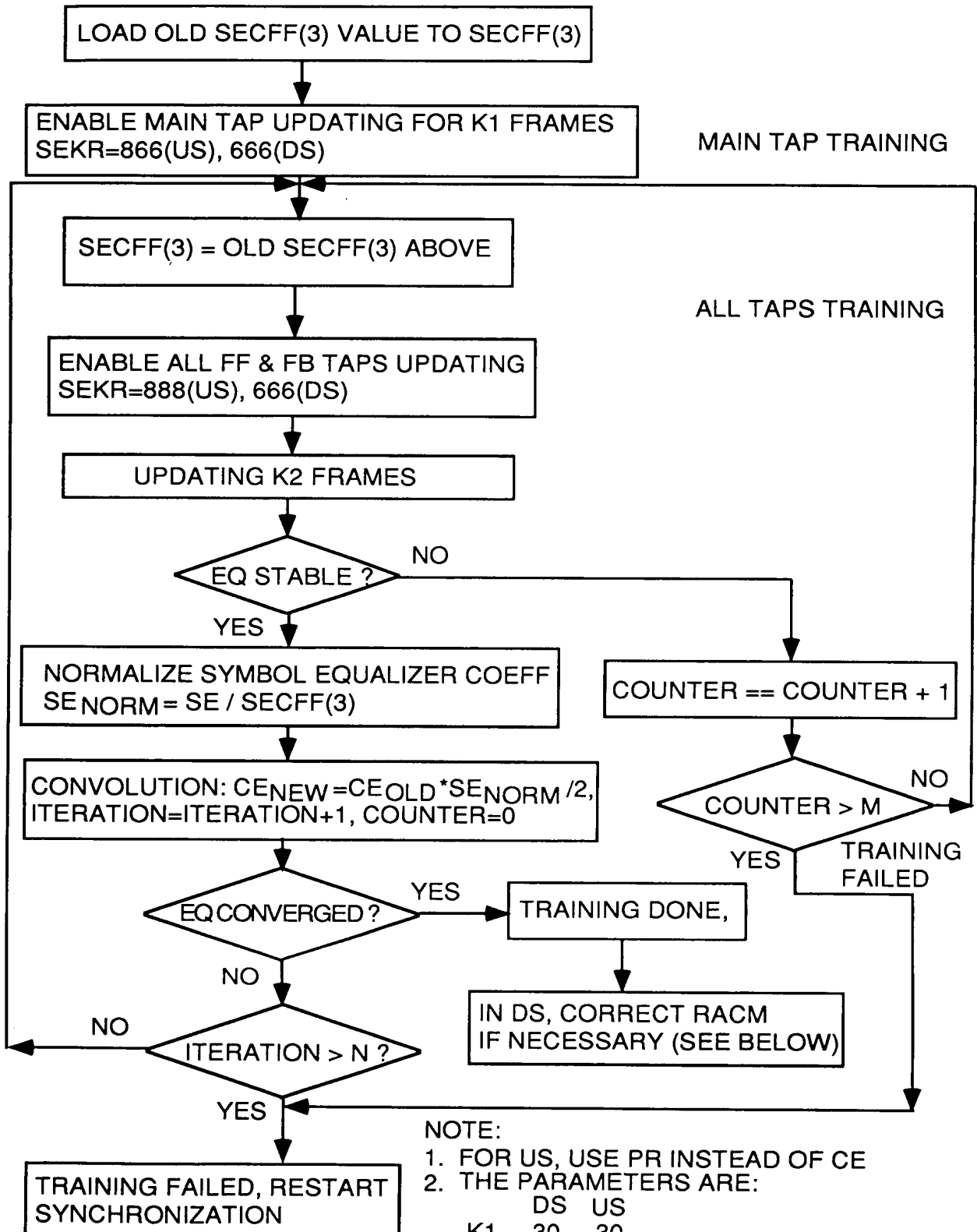
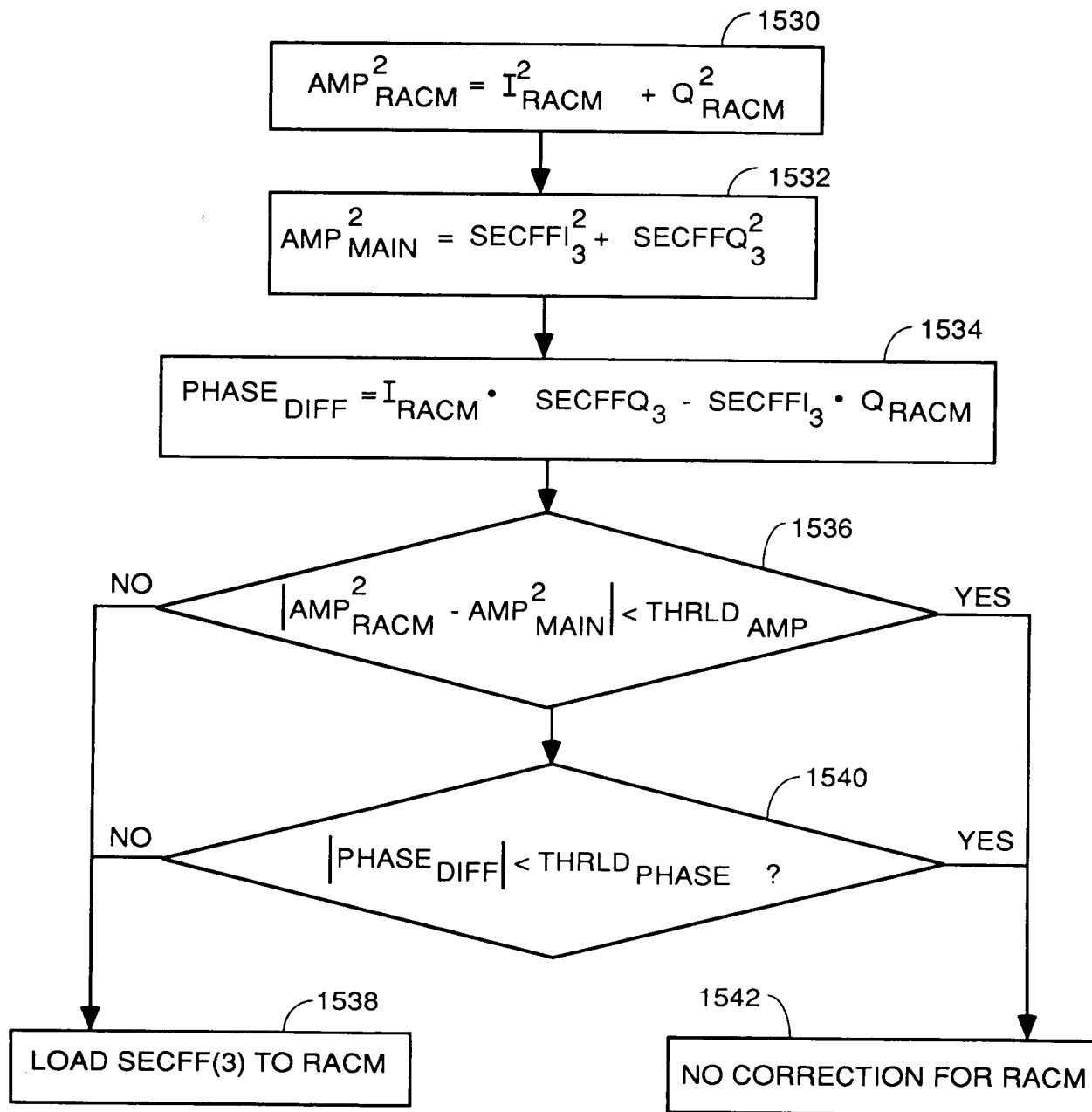


FIG. 62

02740"4265260

RACM CORRECTION



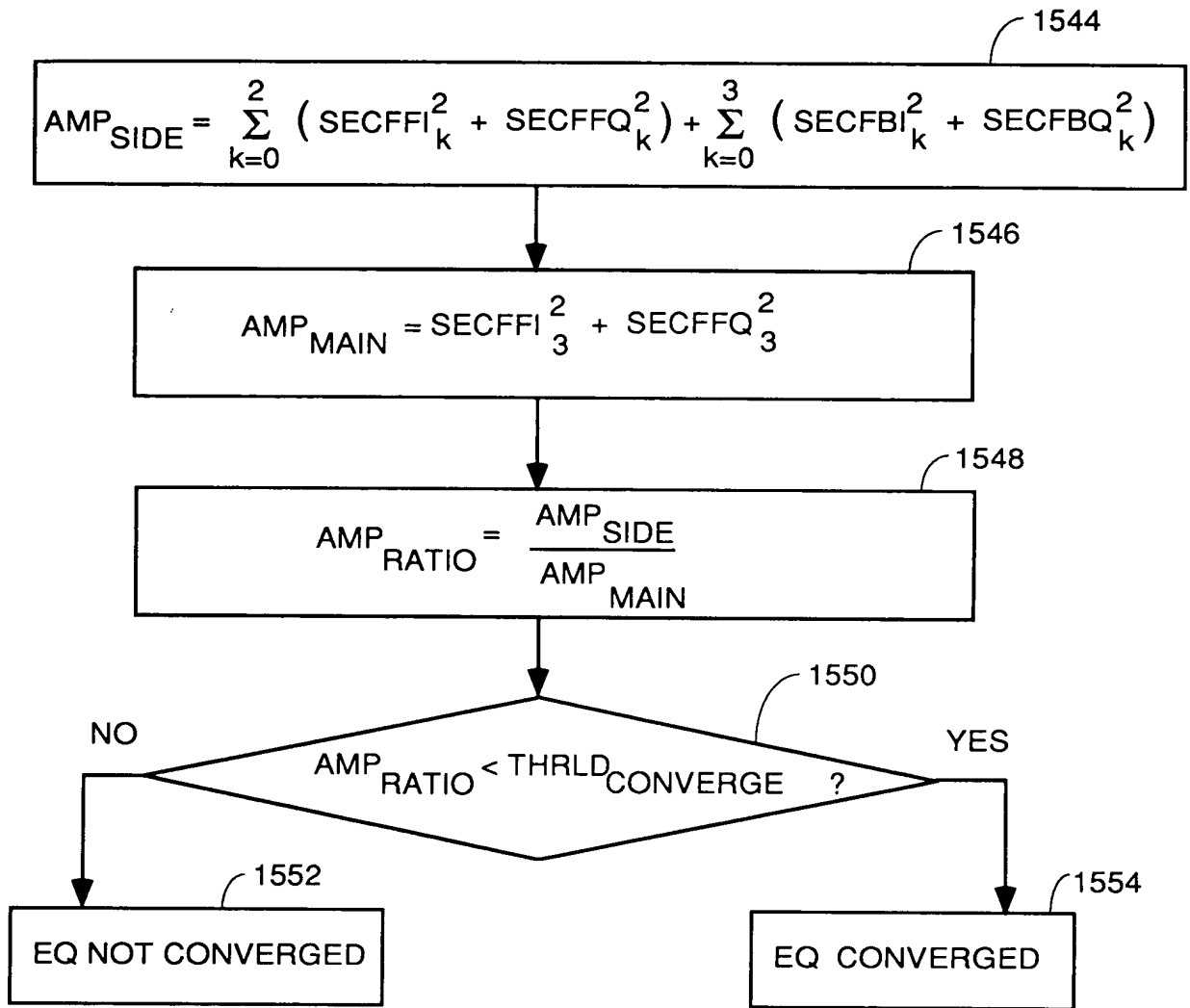
NOTE: THRLD_{AMP} = TBD
 THRLD_{PHASE} = TBD

ROTATIONAL AMPLIFIER CORRECTION

FIG. 63

09759774-04101
 102740-4265260

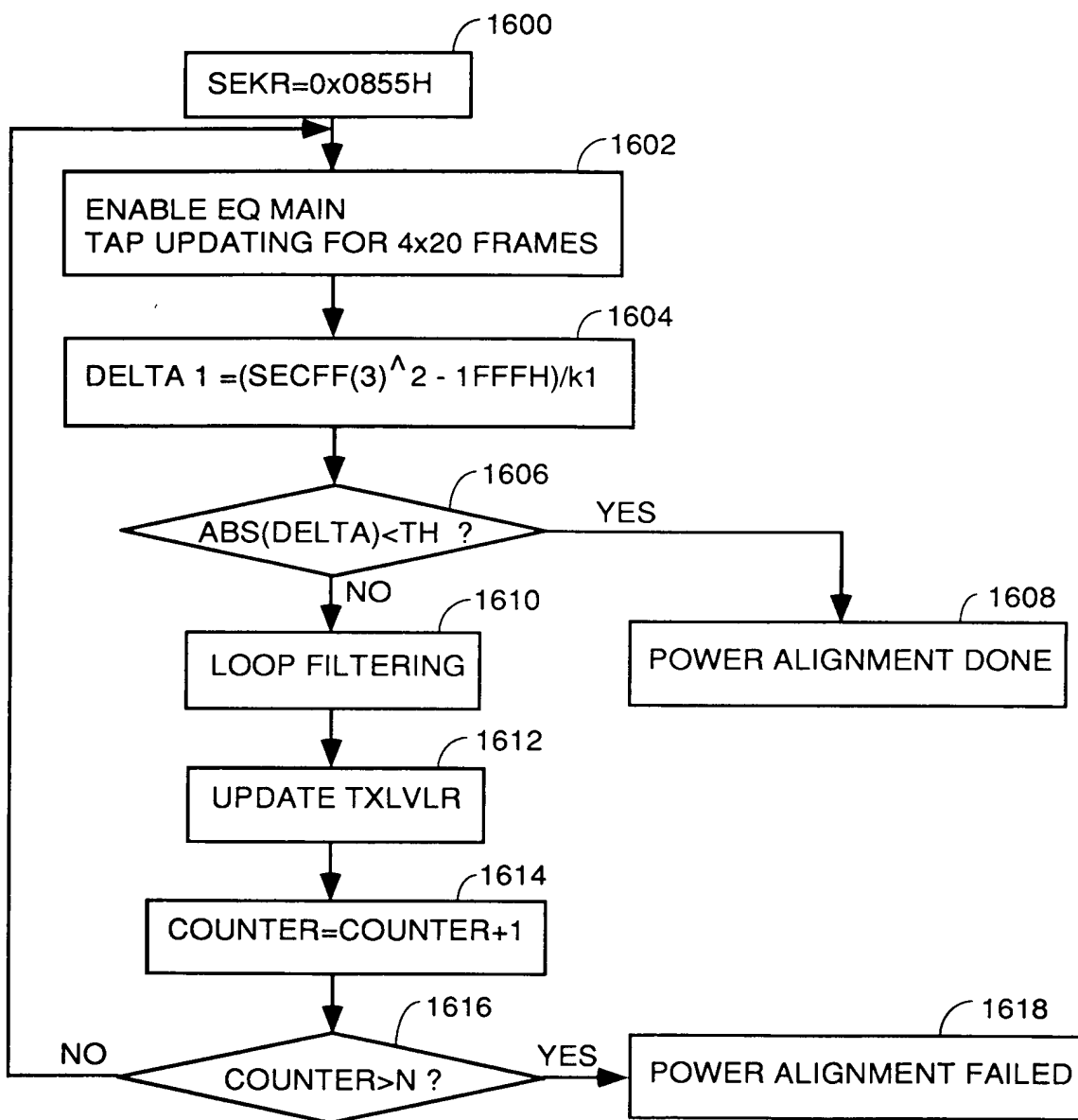
EQ CONVERGENCE CHECK



NOTE: $THRLD_{CONVERGE} = 10^{-5}$

FIG. 64

POWER ALIGNMENT FLOW CHART



NOTE: TH = 600H

N = 12

FIG. 65

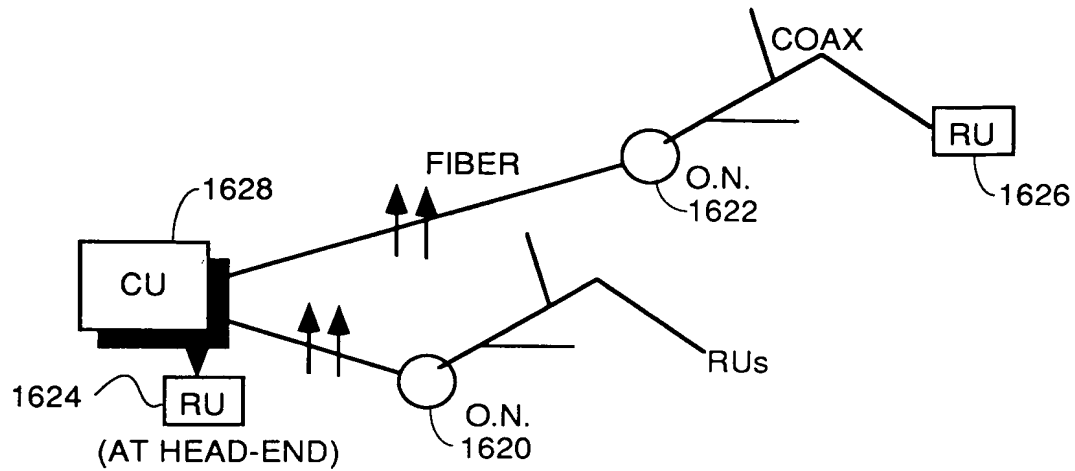
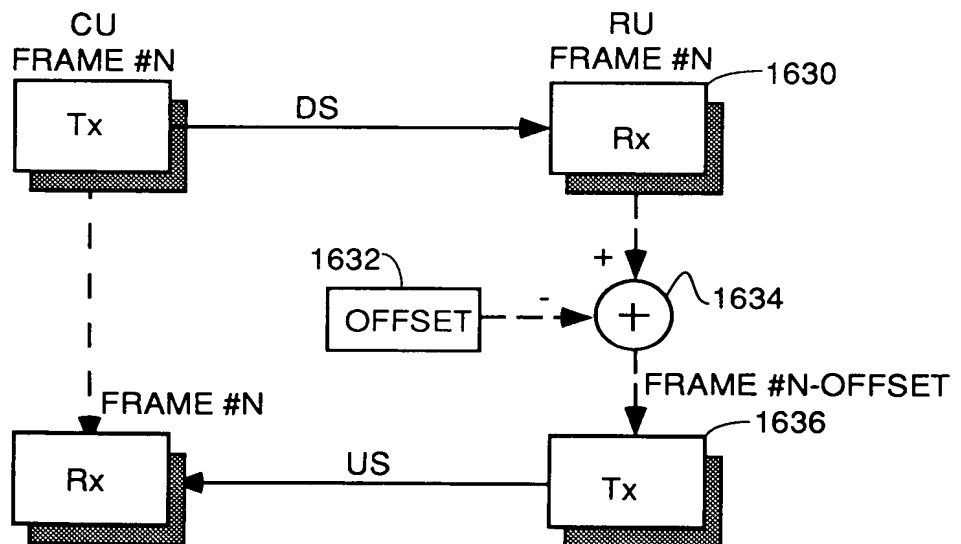


FIG. 66



TOTAL TURN AROUND (TTA) IN FRAMES = OFFSET

FIG. 67

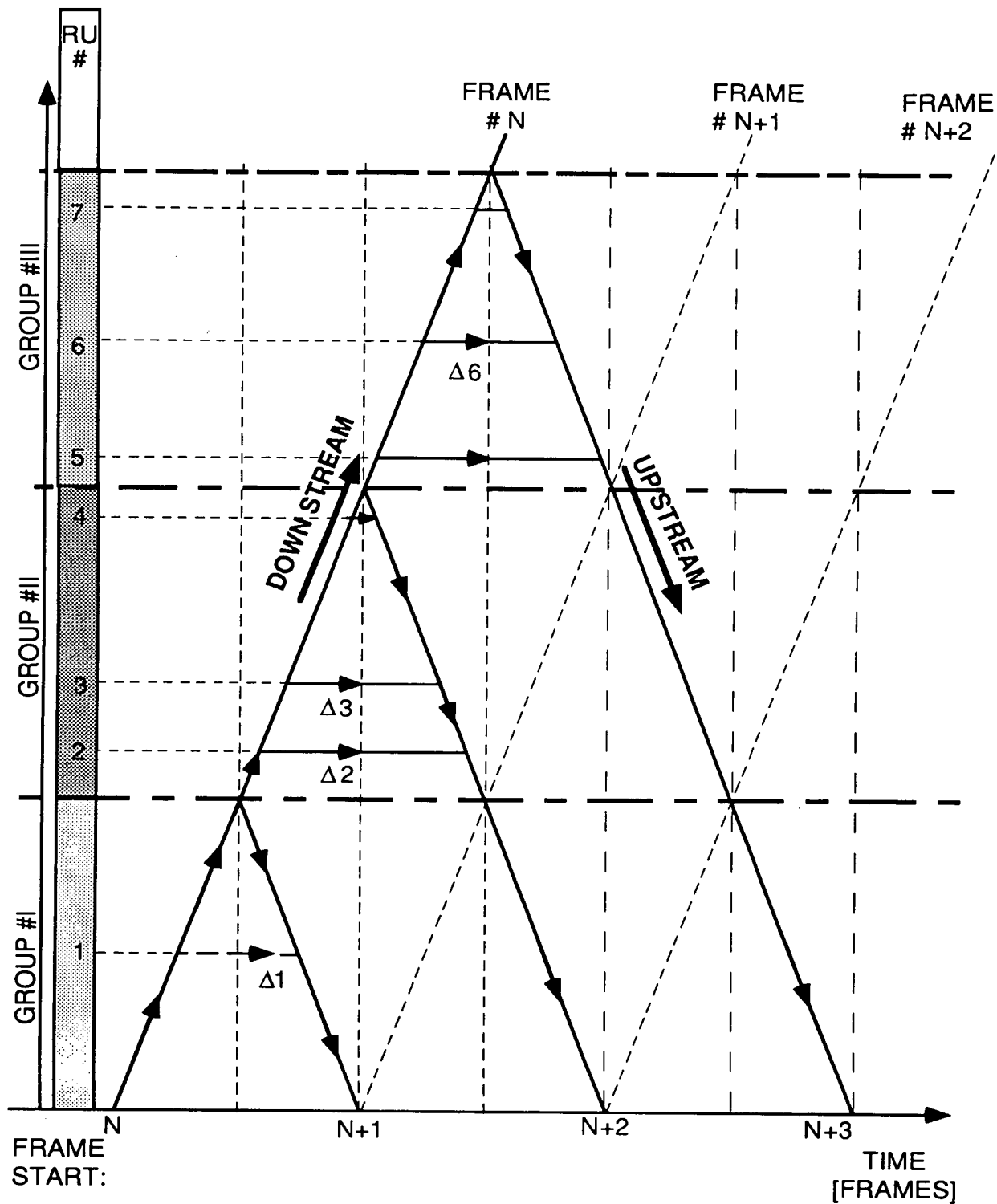
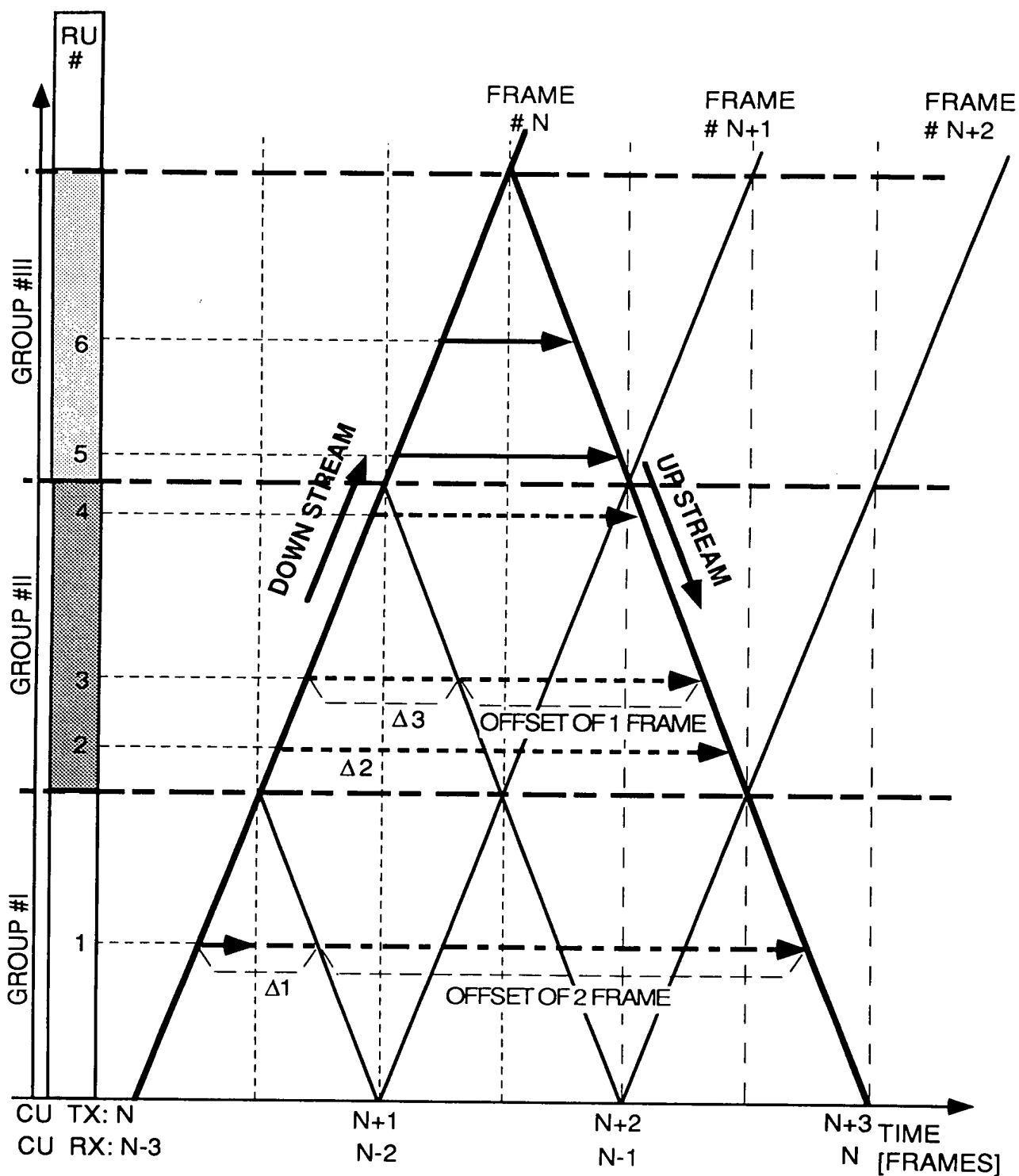


FIG. 68



CONTROL MESSAGE (DOWNSTREAM) AND FUNCTION (UPSTREAM) PROPAGATION IN A 3 FRAMES TTA CHANNEL

FIG. 69

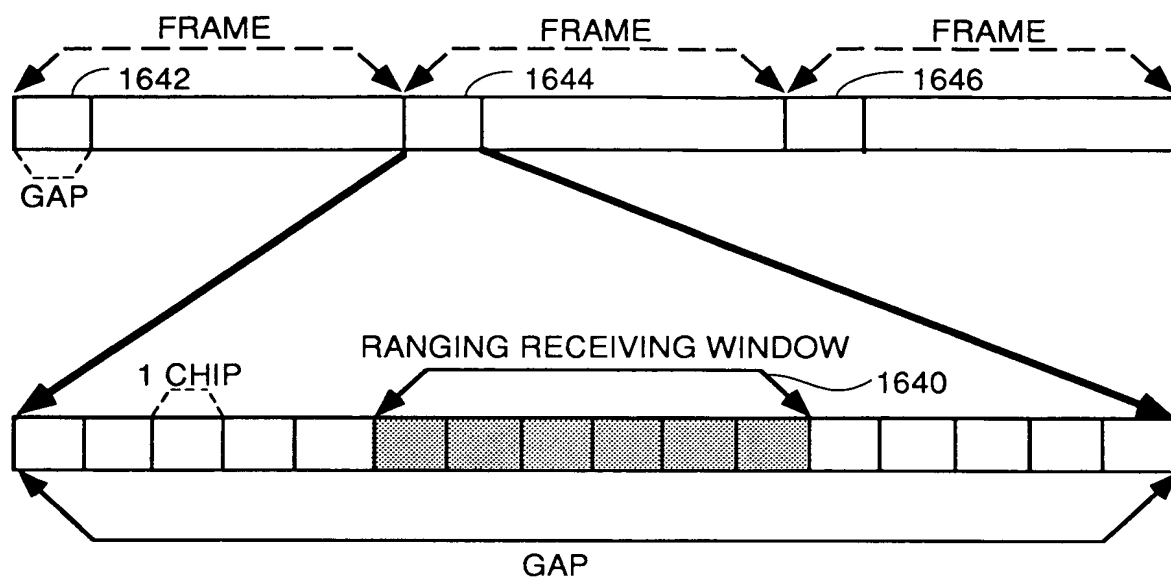
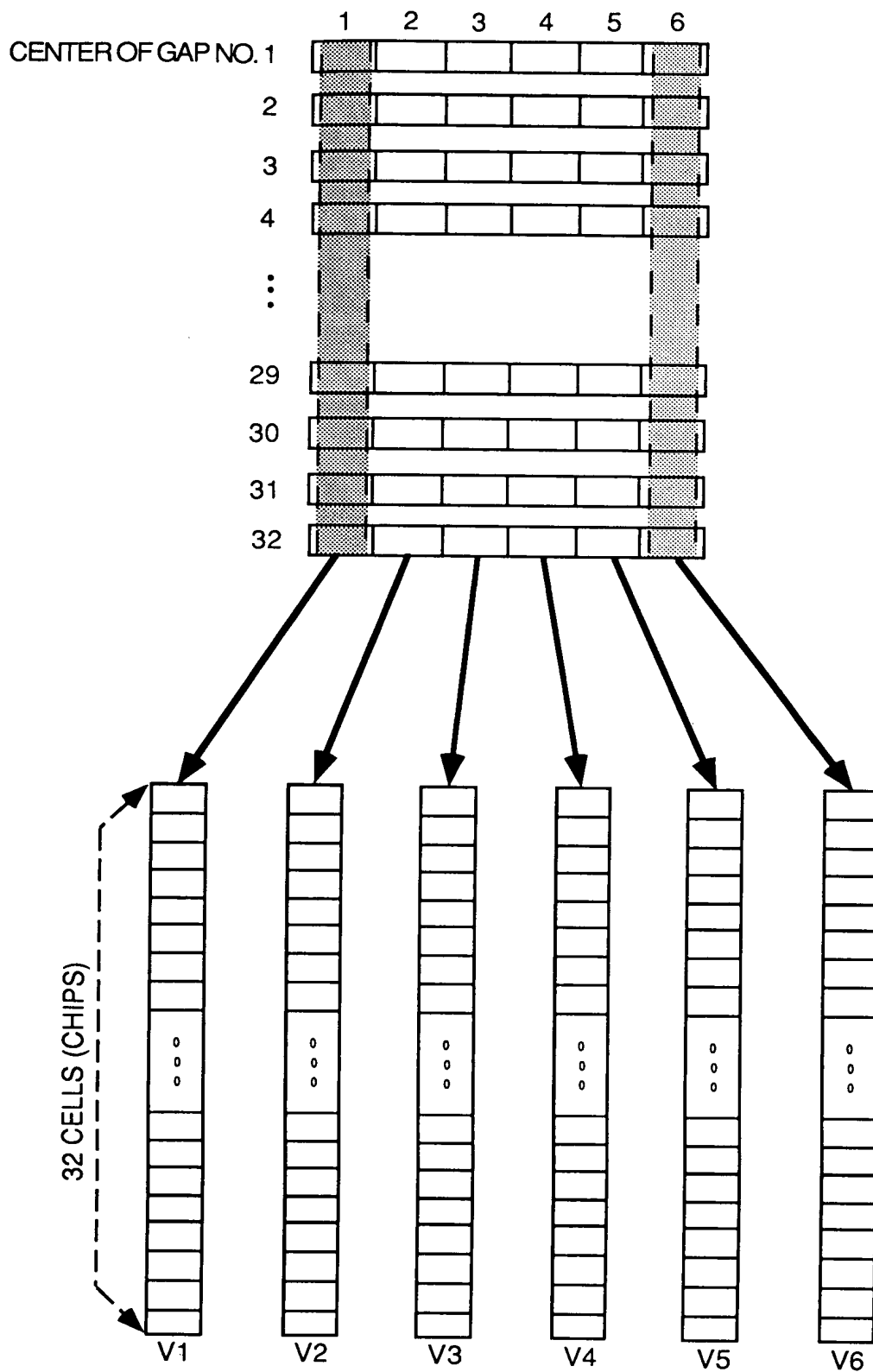


FIG. 70



OVERALL VIEW OF THE CU SENSING WINDOWS
IN A "BOUNDLESS RANGING" ALGORITHM

FIG. 71

095974-041294
F02F40-425560

CHIP\FR	1	2	3	4	5	6	7		33
1	0	0	1	0	0	1	1	...	0
2	1	0	0	1	1	1	1	...	
3	0	0	0	1	1	1			
4	0	0	0	1	0	0	0	...	0
5	0	1	0	0	1				
6	0	0	1	1	1				
7	0	0	0	1	1				
8	0	0	0	0	1	0	0	...	

FIG. 72